U S
University of Stavanger

Faculty of Science and Technology

BACHELOR`S THESIS

Study program/Specialization: Mechanical engineering	Spring semester, 2021 Open
Writer: Ole Kristian Bjørge	*Ole Kristian Bjørge* (Writer's signature)

Faculty supervisor: Professor Vidar Hansen

External supervisor(s):

Thesis title:

Mechanical properties of 316L stainless steel made by selective laser melting using powder produced from recycled scrap material by vacuum induction gas atomizing.

Credits: 20

Key words: *Sustainability* *Selective Laser Melting* *316L stainless steel* *Vacuum Induction Gas Atomizing* *Mechanical properties*	Pages: 49 + enclosure: 12 Stavanger, 29.05.2021

Abstract

The purpose of this study has been to investigate if 316L powder for Selective Laser Melting (SLM) can be made from scrap material by the process of Vacuum Induction Gas Atomizing (VIGA). Unused parts from storage represented 90% of the input material used by the VIGA process to produce suitable powder for SLM and the average sized particle of the powder ended up being 34.30 µm. Then by the use of the so-called "green" powder, the SLM process managed to produce suitable and almost dense (porosity<99.5%) specimens for testing. Further, the characterization of the mechanical properties and microstructure was carried out by performing tensile testing, impact testing, Vickers hardness measurements and light optical microscopy were the porosity also was examined. By investigation of the microstructure, it was found that the microstructure exhibited similar characteristics found in other studies studying SLM manufactured 316L specimens. These similarities include observations of overlapping melt pools due to partially remelting, what is believed to be epitaxial grain growth as well as grains growing in no preferred direction. Thus, indicating that the laser scanning pattern has successfully manage to create isotropic like conditions in the microstructure. Overall, the microstructure seems to correspond well with the achieved mechanical properties and as can be normally observed with regards to SLM produced specimens, exhibited the z-oriented tensile specimens lower yield and tensile strength. However, the mechanical properties generated by tensile testing where all within the requirements of the relevant standard, though they exhibited slightly lower properties than the specimens produced by regular powder. Which is most likely due to the chemistry being slightly different in the finished specimens of this study compared to the ones produced by the regular powder. The tensile specimens in x-, y- and z-direction of this study exhibited tensile strength of 619.1 (x), 631.1 (y) and 554.2 $\pm$ 6.35 (z) and yield strength of 519.3 (x), 541.9 (y) and 455.8 $\pm$ 2.45 (z) respectively. Therefore, it can be concluded that it is feasible to produce 316L powder, suitable for Selective Laser Melting (SLM) by the use of scrap material as the main input material when producing powder by Vacuum Induction Gas Atomizing (VIGA).

Acknowledgment

Directory of abbreviations

AISI	American Iron and Steel Institute
AM	Additive Manufacturing
ASTM	American Society for Testing and Materials
BCC	Body-Centered Cubic
BF-BOF	Blast Furnace-Basic Oxygen Furnace
CNC	Computer Numerical Control
E	Young's Modulus
EAF	Electric Arc Furnace
EL	Elongation
FCC	Face-Centered Cubic
L-PBF	Laser Powder Bed Fusion
PSD	Particle Size Distribution
ROA	Reduction of Area
SD	Standard Deviation
SEM	Scanning Electron Microscope
SLM	Selective Laser Melting
SLS	Selective Laser Sintering
SS	Stainless Steel
UTS	Ultimate Tensile Strength
VIGA	Vacuum Induction Gas Atomizing
VIM	Vacuum Induction Melting
YS	Yield Strength

Innholdsfortegnelse

1 Introduction

In the recent time recycling has been gaining the attention of both the public and industrial sector. Why recycling has gained all this attention has a lot to do with sustainability and the goal to achieve a circular economy. Circular economy is briefly explained when a part is recycled and made into a new part instead of being thrown out. An easy way to do this on paper, and which can be seen in Figure 1, is simply to recycle a part, make powder of it, design a new part, 3D-print a new part and finally, put the part to use. As said, on paper this sounds easy, but in reality, there are a few challenges to say the least. These challenges will be briefly addressed later.
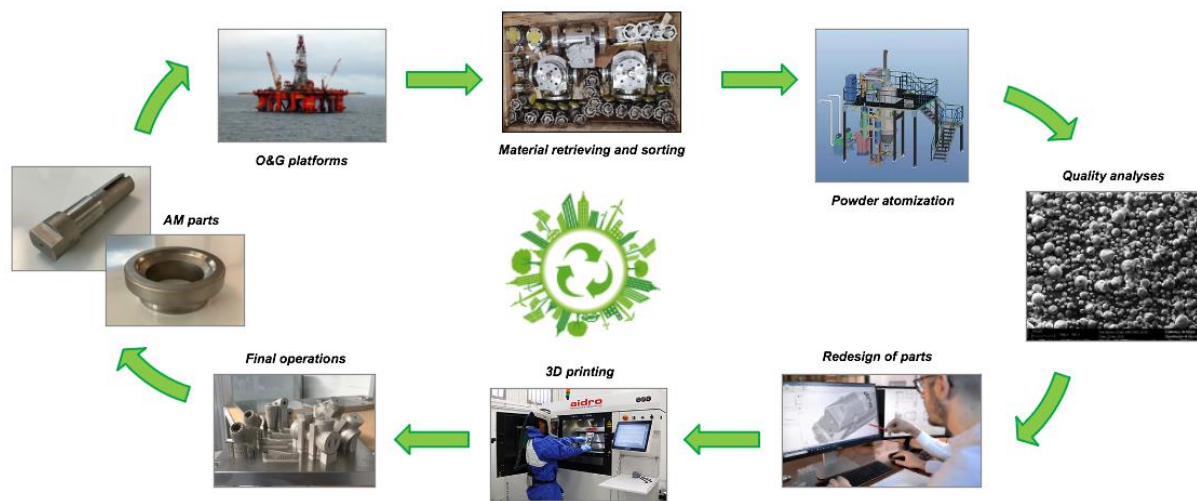
Figure 1: This proposed circular economy is proposed by the company F3nice.

First, what then is so desirable about a circular economy? It could be the fact that a circular economy leads to an optimal resource efficiency, which businesses tend to find very desirable, especially considering economics. How then is an optimal resource efficiency achieved? It is achieved when as little material as possible is used to produce a part without impacting the mechanical integrity of the part and there being little to no waste material when the part is finished. As it happens these two key factors are also two of the advantages of additive manufacturing. Therefore, it could be desirable to incorporate Additive Manufacturing (AM) into a circular economy, as F3nice wants to do. Additive Manufacturing is a process where three dimensional objects are produced, usually layer by layer which allows for complex designs that could be near impossible to produce any other way.

As one can see in Figure 1 the part has to be recycled to achieve the proposed circular economy. Briefly explained, recycling is to take something that can no longer be used and turn it into

something that can be used. Practicing recycling adds both some advantages and disadvantages and in an economic and environmental perspective the advantages are very attractive. The question then becomes, does the advantages outweigh the disadvantages, but in order to answer that the material has to be specified. Which brings us to stainless steel, the material being used in this study, which can even more generally be defined as steel. The reason for this generalization is because the raw material used to create the metal powder will be referred to as steel scrap in this study. Though it has to be mentioned that stainless steel has a major advantage of more or less remaining uncontaminated when exposed to the environment and this makes it very practical to recycle.

As mentioned earlier there are some environmental and economic advantages of recycling steel. The main advantage on the environmental aspect of recycling steel does not come from any pollution that stainless steel might do when left in the environment, but from the production of steel. The reason why is because steel is mainly recycled by the use of an Electric Arc furnace (EAF), which uses significantly less energy and releases significantly less CO_2 than a Blast Furnace-Basic Oxygen Furnace (BF-BOF). This will be elaborated in the literature study.

The other advantage is as mentioned the economic aspect. The economic advantage arises as a result of the environmental advantage. The use of less energy and lower emissions usually results in lower costs and by using a renewable energy source the emissions can be further lowered. Another advantage on the economic aspect is that scrap material costs less than new material at this moment in time. However, it has to be mentioned that the less expensive scrap material is scrap categorized as retrievable. Yes, in theory steel is 100% recyclable, but in reality, with current technology, this is not the case. This was pointed out by a study done in 2015 (Bratkovich et al., n.d.). The study pointed out that the amount of steel that is actually recycled is lower than what is reported. This is actually positive because it means that there is an even greater amount of steel that potentially can be recycled compared to what has been reported. The reported numbers the study assessed came from Steel Recycling Institute, U.S. Geological Survey and Canadian Steel Producers Association. The numbers had a lot of variation and the study explained this by a difference in how steel scrap is categorized. Further the study addresses the problem of recovering steel, which brings us to the disadvantage of recycling steel. Said in another way, a problem with the recycling of steel, because it is not permanent and in the future as technology advances it may be possible to recycle steel that has been deemed unrecoverable.

What exactly then makes some steel deemed as unrecoverable and where does the difficulties in the recycling process come from? According to (Damuth, 2011) the reason why some steel is unrecoverable is twofold. Firstly, there is the fact that some steel is lost through corrosion, wear, and tear and secondly some steel is discarded in a manner or place that does not allow for recovery. When it comes to difficulties in the recycling process the main problem is contaminations. By contamination it means unwanted substances in or on the material being recycled. Contaminants affect the mechanical properties either in the present state like rust in form of oxidation or further down the line in the finished product. Therefore, these contaminants must be properly removed in order to obtain the desired mechanical properties of the finished part. Especially with regards to 3D-printing where small deviation in chemistry can notably affect the finished product. One type of contaminants can be that the steel is mixed with or coated with other materials such as plastic and glass. Another can be the presence of metallic and non-metallic substances within the steel, which is the most difficult to deal with. Unwanted elements within the chemistry can in many cases be very difficult to remove and, in some cases, impossible with current methods and technology. This problem leads us to the proposal of F3nice to further cut costs, emissions and time.

In order to further increase the advantage of using steel scrap, F3nice has gone one step further and proposed and patented the approach in Figure 2.
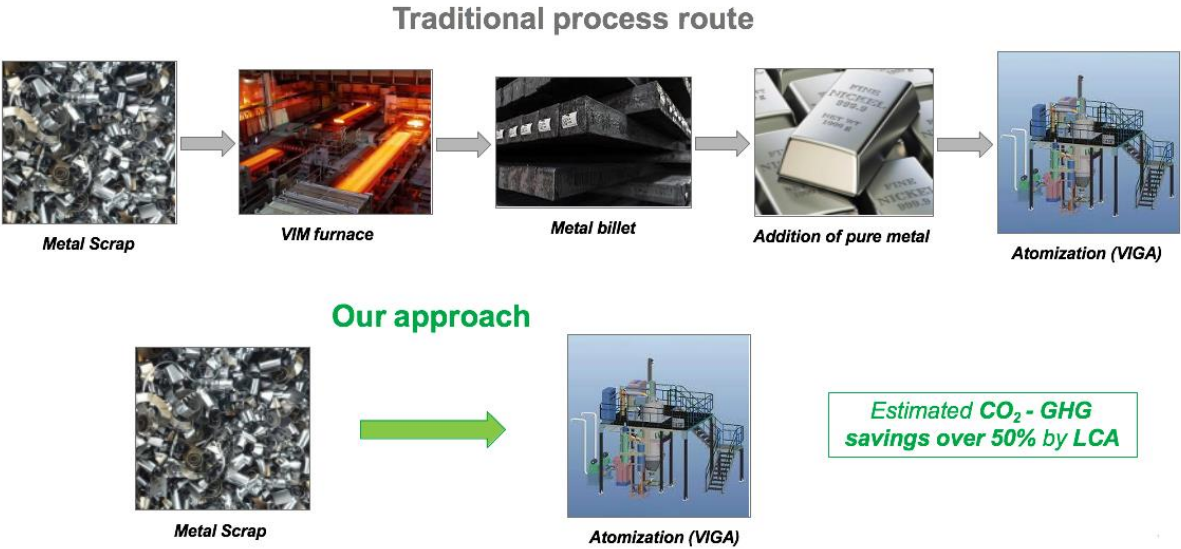
Figure 2: F3nices proposal to a new supply chain model.

What they are proposing is not to skip the step of sending the steel scarp to an Electric Arc Furnace (EAF) for processing, but to merge the process into one step. Where the steel scrap is used as the raw material to make metal powder for AM by Vacuum Induction Gas Atomizing

(VIGA). Why this is a realistic and very reasonable proposal will be elaborated on the literature study. It has to be mentioned that as one can see in Figure 2 the furnace used is called VIM, which stands for Vacuum Induction Melting and is a subcategory of EAF. VIM is a very suitable process to use when producing stainless steel, but in the literature study the term EAF will be used as its referrers to all types of electric furnaces.

Therefore, with the recently discussed problem of contaminants within the chemistry in mind, it becomes relevant to investigate if 316L powder for Laser Powder Bed Fusion (L-PBF) can be produced by Vacuum Induction Gas Atomizing where the raw material is steel scrap. In this study the mechanical properties of the 3D-printed parts will be assessed and compared with industrial standards.

2 Literature study

2.1 Steel production

Today, steel is mainly produced in two ways. One is by the Blast Furnace-Basic Oxygen Furnace (BF-BOF), also called the "primary" path, because usually new or so called "virgin" steel is produced this way by the use of iron ore, coal and limestone. The other one is by Electric Arc Furnace (EAF), which is often called the "secondary" path, because this way of producing steel usually uses steel scrap as input material.

A few numbers:

- BF-BOF accounts for around 70% of the world's steel production(*Worldsteel | Worldsteel*, n.d.)

- EAF accounts for around 30% of the world's steel production(*Worldsteel | Worldsteel*, n.d.)

- EAF accounts for as much as 80% of the world's stainless steel production(*Stainless Steel and CO2: Facts and Scientific Observations*, n.d.)

The Electric Arc Furnace (EAF) is also the process that is usually used to recycle steel scrap. This is because the EAF process has the ability to reach a higher temperature and therefore it has a better capability to remove unwanted elements associated with steel scrap. In fact, up to 100% scrap can be used as input material in an EAF compared to BOF where only 30-35% of the input can be scrap. The point is that EAF is the primary process in order to recycle steel scrap and is also the primary process for producing stainless steel. Therefore, it is relevant to look at this process when recycling stainless steel, especially because the first stage in a gas atomizing process is technically an EAF process or more precisely a VIM furnace.

2.1.1 Electric Arc Furnace

The Electric Arc Furnace utilizes the fact that it uses on average 60% less energy and 70% less carbon dioxide is released compared to production by iron ore(*Grønnere – Stålproduksjon i dag*, n.d.). It also takes advantage of the relatively low price of steel scrap. This may change in the future in the event of an increase in demand for scrap steel, especially considering the increased focus on recycling.

Briefly explained the first step in the electric arc furnace process is to put scrap material and other relevant materials into the crucible. Which materials that are put in and the amount depends on what the desired chemistry is. Then electricity is applied to the crucible and a current is used to melt the metal. When the metal is fully melted the chemistry is controlled and relevant materials may be added. Then when the chemistry is as desired the production continues to the next step. If it was a VIM furnace the main difference would be that the melting happens under vacuum and on a smaller scale. This allows for a higher degree of control of the chemistry and there are low environmental contaminants. The final step is the casting and the result from this step is usually a slab, billet or bloom. Which is either shipped or further processed. Then, if you for example wanted to make metal powder by gas atomizing from a steel slab. The slab would reenter a melted state once again.

2.2 Stainless steel

Stainless steel is considered a "green" material mainly because of its excellent recyclability. This comes from the fact that stainless steels are very corrosion resistant when in a solid state, which results in almost no contaminations when in contact with other elements. In other words, the chemistry is more or less preserved which makes the recycling process a lot easier to manage. Stainless steel is also very desirable to recycle because it contains many valuable alloying elements. Different alloying elements are added in order to achieve desired mechanical properties depending on its use. One of them is chromium, in fact every stainless steel contains at least 10.5% chromium (*The Stainless Steel Family*, n.d.), because this is what makes the steel stainless by creating a passive film when in contact with oxygen in air or water. Another alloying element that may be added in order to further enhance corrosion resistance, is molybdenum. Which brings us to the steel in question, American Iron and Steel Institute graded 316L.

2.2.1 AISI 316L

AISI 316L is an austenitic stainless steel which is made suitable for welding and AM by reducing the carbon content of AISI 316, thereby getting the name 316L where the "L" is signifying the low carbon content. A low carbon content reduces the risk of sensitization which can occur if the material is exposed to a sufficient amount of heat for a long time. Another feature of this steel which distinguishes it from other stainless steels and makes it very suitable for applications exposed to chloride environments is the addition of molybdenum.

Table 1: Chemical Composition of AISI 316L(wt %)(ASTM International, 2016)

ELEMENT	C	MN	P	S	SI	CR	NI	MO	FE
MIN	-	-	-	-	-	16.0	10.0	2.00	Balance
MAX	0.030	2.00	0.045	0.030	1.00	18.0	14.0	3.00	

There are four significant elements that play a major role in giving this steel its mechanical properties and microstructure. They are chromium, nickel, molybdenum and carbon. As seen in Table 1 the first three also make up the biggest percentage except iron.

The effect of major alloying elements in 316L:

- *Chromium:* As mentioned above chromium has to be added in order for the steel to be a stainless steel. The reason it is added is because of its strength and its high corrosion resistance. When a sufficient amount of chromium is added to the steel a passive film is created on the surface. This film is very thin, but it reduces the corrosion to negligible levels. The film is also self-repairing, which means that the film will repair itself should the surface for example be scratched.

- *Nickel:* This element has an austenitic structure and when added it helps promote an austenitic structure compared to chromium which promotes a ferritic structure. In fact, a sufficient amount of nickel has to be added in order for 316L to form an austenitic structure at room temperature. Therefore, nickel is considered an austenite stabilizer and its addition improves the ductility and toughness of the steel, especially at high temperatures. It also has some corrosion resistance in sulfuric acid environments and Nickel has no direct influence on the passive film.

- *Molybdenum:* The fact that molybdenum has a very high melting point helps to improve the strength of the steel at very high temperatures. As mentioned above the addition of molybdenum improves the resistance to corrosion. More specifically to pitting in chloride environments and crevices in both Fe-Cr and Fe-Cr-Ni alloys. Molybdenum also influences the passive film in that it ensures the passivity by reducing the intensity of the oxidizing effect and reduces the tendency of formed films to break down.

- *Carbon:* This element is found in every stainless steel. It is added in order to obtain high strength and hardness. Carbon is also a very strong austenitizer. Despite this the carbon content in 316L is very low and that is one of the characteristics of this steel because it makes it very suitable for welding and AM. The reason why the carbon content is very low is because when carbon is mixed with chromium it can lead to formation of

chromium-carbide. This can again have a very significant negative effect on the passive film because of a reduced availability of chromium.

2.2.2 Microstructure

All metals have crystallin structures because of the amount of stabilization achieved by adopting a crystalline arrangement. The stabilization comes from the fact that a particle has a preferred position in relation to other particles, thereby adopting regular (rather than random) arrangements. A single crystal can be categorized by having a repeating arrangement of atoms or molecules. It is then possible to specify the crystal structure by describing a small representative arrangement of atoms called the unit cell. There are several types of unit cells, but common for metals are the Body-Centered-Cubic (BCC) and Face-Centered-Cubic (FCC) unit cell and it is these that determines the phase of the solid. With regards to stainless steels, if it were determined that after solidification the steel has an FCC unit cell, it is then said that the steel has an austenitic phase. Then, when solidification starts, the atoms start to arrange themselves and form a crystal and this formation will not only start at one place, but in many places at once. Then as the metal solidifies the crystals grows until they hit another crystal with a different orientated structure. These different oriented crystals are what is called grains and where they interact is called the grain boundaries. The number of grains that are formed, the size of them and the phase strongly depends on the alloying elements of the metal and the temperature during the solidification. The size of the grains and the structure within the grains strongly influences the mechanical properties of the metal and by changing any of the two factors the mechanical properties can be changed. The reason why the grain size matter is because of the degree of freedom of movement the dislocations gets as a result of the size.
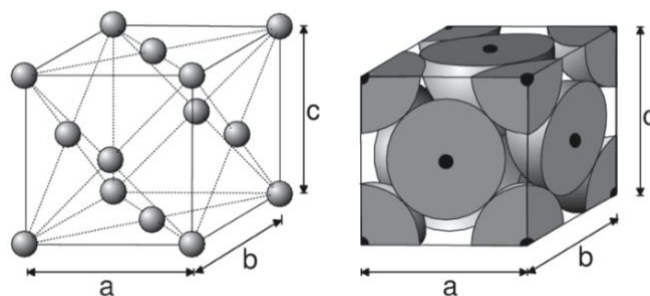

Figure 3: FCC unit cell. ("alfajern," 2020)

2.2.3 Dislocations

It so happens that a perfect crystal structure with every atom in place does not exist. In fact, the case is that every single crystal happens to have defects. Defect may be a negatively loaded word, but it is defects that give strength to the material and one type of defect are dislocations.

Briefly described, dislocations are when the atoms are not located inside their equilibrium positions but are displaced relative to these equilibrium positions. Generally, there are two types of dislocations, edge and screw dislocation. Common for both of them is that they have to move when the material is exposed to a force. A dislocation will always move in the least energy demanding direction and that is usually along the most closely packed plane and preferably within the same grain. The reason being is that it is not very energy demanding to break atomic bonds compared with moving across grain boundaries, which is what really stops any movement. The reason why moving across grain boundaries is highly energy demanding is because of the neighboring grain having a different oriented structure. Therefore, as above it can be said that grain size matters because a bigger grain will allow a higher degree of low energy movement, but will on the other hand lower the strength, ductility and hardness (*Nondestructive Evaluation Physics : Materials*, n.d.). With regards to 3D printing fusion lines will also act as grain boundaries and prevent movement.
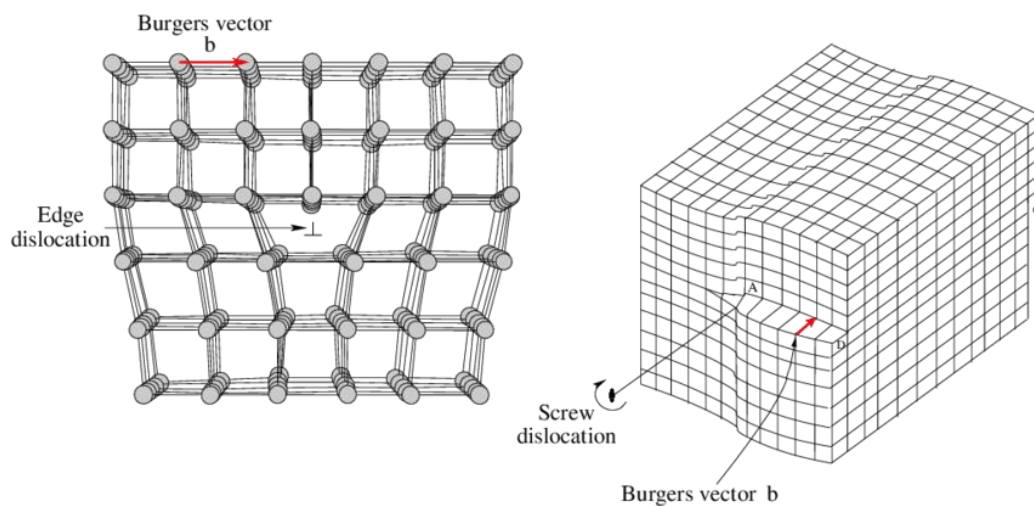

Figure 4: Schematic diagram of edge and screw dislocation. (González-Viñas & Mancini, 2003)

2.2.3 Austenite

The micro- and macrostructure of AISI 316L is as mentioned austenitic. The reason why this structure is often desirable is because in general austenitic stainless steels are considered to have the overall best corrosion resistance(Smith, 1993). Another way to look at it is that a ferritic structure is often unwanted, because long-term exposure of this structure at elevated temperatures can lead to reduced ductility, toughness, pitting resistance and crevice corrosion resistance(Sedriks, 1996). Which is usually unwanted mechanical properties, but under controlled conditions the presence of ferrite can be used to obtain certain wanted mechanical properties. Ferritic structures also happen to be magnetic because they have a body-centered-cubic (BCC) structure compared to austenite which is nonmagnetic because it has a face-

centered-cubic (FCC) structure. This is a point worth noting because metal scrap being recycled is often collected with the help of magnets. On the other hand, it is possible to find out if the structure is entirely FCC by the lack of magnetic attraction. Though a major disadvantage of austenite is the occurrence of sensitization which can lead to intergranular corrosion.

2.2.4 Corrosion

Corrosion can be defined as the dissolvement of refined materials because of natural reactions with the surroundings which converts it to a more stable form. In AM by AISI 316L there are two very relevant corrosions to look at. One is pitting corrosion and the other one is intergranular corrosion. The commonality of these two corrosions is that they both can be caused by sensitization. As mentioned earlier sensitization is a problem that can occur when both carbon and chromium are included in the chemistry, but in order for sensitization to occur certain conditions must be present. These conditions happen to be present in welding and AM production. Though AISI 316L has a very low carbon content, sensitization can still occur.

A brief explanation of pitting and intergranular corrosion

- *Pitting:* This phenomenon is most easily explained by the formation of pits, hence the name. Pits form when in contact with the surroundings and can be very destructive in a structure if it causes perforation of equipment. In AISI 316L chromium, nickel and molybdenum are the main preventers of pitting. Among other things the passive film created by chromium is very important in preventing pitting.

- *Intergranular:* This form of corrosion takes place on the grain boundaries and the main cause is sensitization. What happens is that chromium carbide is formed on the grain boundaries. This leads to chromium depletion on the grain boundaries, but not within the grain. What follows is formation of something that looks like cracks, but the grains become easy to observe.

2.3 The Powder

Metal powder is not just metal powder. It is like gravel, it comes in various shapes and dimensions, but a lot smaller in size. What properties the powder has depend on its end use. Since metal powder has been around the industry for a long time its use can be found in many sorts of products. Among other things the use of metal powder can be found in the making of metallic paint, batteries, brake pads and in recent time, in AM. In AM there are very specific

properties required and especially in L-PBF. From literature it is also known that small deviations in the chemistry can have a noticeable impact. (Cacace et al., 2020)

2.3.1 Wanted properties of metal powder
In general AM-technologies requires powder that:

- Is spherical shaped
- Satellite-free
- Has the highest attainable packing density
- Has a specific Particle Size Distribution (PSD)
- High flowability
- Density
- Has an internal particle structure which is free of pores

As said different AM technologies require different degrees of the listed requirements above, but probably the most important property is the spherical shape. Note that it is not that the powder must be as spherical shaped as possible, but it has to be spherical shaped. According to the author of (*Metal Powders for AM*, 2018) it is a misconception that the goal is to achieve the most spherical powder as possible. He rather states that non-spherical powder is unsuitable for AM production. Why is sphericity so important? The reason why sphericity is so important is by achieving this property combined with a good Particle Size Distribution (PSD) many of the other properties are achieved simultaneously. By a good PSD it means a particle size distribution that is normally distributed.

Normal distributed spherical shaped particles lead to:

- Good flowability (powder feeding) – smoother layers in L-PBF
- Improved packing density
- Increased heat conduction in the powder bed
- An enhanced melting profiles

An advantage of spherical particles where the PSD does not matter is the fact that spheres have a lower surface area compared to volume than other shapes. This leads to a lower exposure to the environment, which is very desirable considering contamination.

2.3.2 Effects of sphericity and Particle Size Distribution

L-PBF is the AM technology that requires the finest powder, and a typical PSD would be 15-60µm. The reason why PSD is so important is that a good combination of different sized particles makes the packing density very high and improves the flowability. Just imagine trying to pack together the same sized marbles. There would probably be some room left, but by introducing smaller marbles the leftover rooms could be filled. In other words, a good PSD will result in a good packing density especially if the particles are spherical shaped. It is also useful imagining marbles when thinking of flowability. What flows best? Marbles or gravel? Good flowability is important in order to prevent any plugging in the machine and to keep the process going. Flowability is also improved by the existence of the right number of the smallest particles, but too many will reduce the flowability. The small particles also melt quickly which improves the heat conduction and melting profile, but the smallest particles also evaporate more easily creating smoke and porosity. To sum it up sphericity and PSD are important factors when making powder suitable for AM and gas atomizing is a good way to achieve those properties when the material is 316L.

2.4 Powder Bed Fusion

Powder bed fusion refers to a set of different AM technologies. This includes Direct Metal Laser Sintering, Selective Laser Sintering (SLS), Electron Beam Melting, Multi Jet Fusion and Selective Laser Melting (SLM). Common for all of them is the use of a powder bed where the particles are combined together with the use of heat. The amount of heat that is applied, determine if it is a melting or sintering process. Take SLS and SLM, which are two technologies that are often confused with one another. The difference is that in SLM the powder is completely melted, in other words it goes through a phase change, from solid to liquid and then solid again. While in SLS the powder is heated to the point where the particle surfaces are melted together to form one solid body. This is a very important difference because it leads to a difference in mechanical properties. The reason for the difference is because particles are limited in their capacity to totally fill up all the available space. While it is well known that a liquid fills up every available space. This results in there being many small pockets within the finished part, which is filled with gas and affects the mechanical properties. It has to be said that sintering requires a significantly lower temperature compared to melting and that takes away the risk of changing the microstructure that was achieved when the powder was made. A change in the microstructure can as explained earlier have a significant impact on the mechanical properties. Therefore, SLM has to be properly managed with respect to temperature

and cooling rates. Though controlled properly SLM is the process that can achieve the best mechanical properties of the two and is also the one used in this study.

2.4.1 Selective Laser Melting introduction

Selective laser melting is a very attractive process, because it can produce parts with very complex designs and at the same time achieve equivalent properties that of industrially produced parts. The reason for this is because SLM is the technology that has the thinnest layers in the industry resulting in the part being divided into the greatest number of layers.
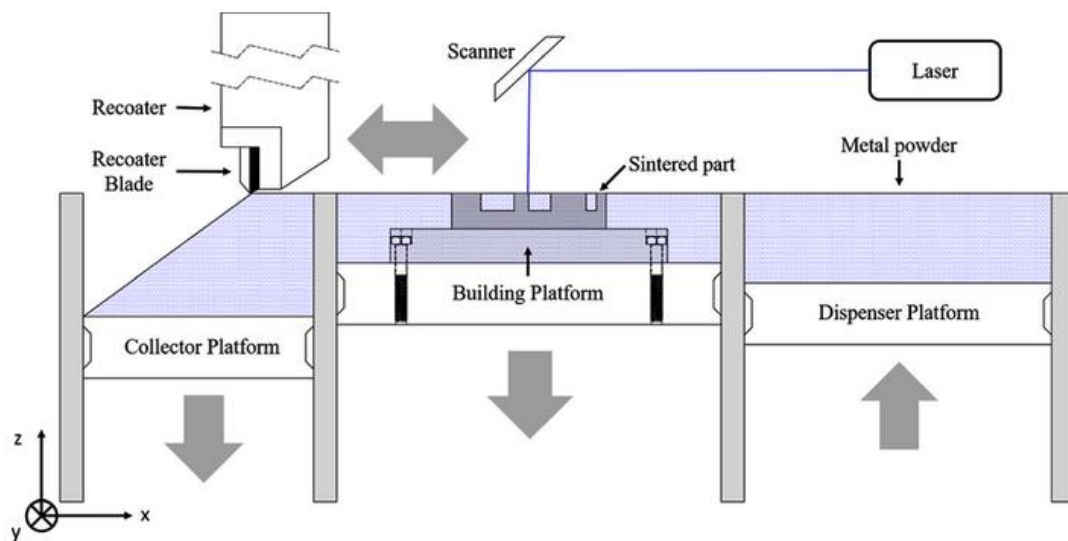

Figure 5: Schematic based on an EOS 290 machine. (Guo et al., 2021)

The process begins by the coater spreading a layer of powder across the build platform. Then the laser selectively melts the powder according to a 2D slice of the part. The platform is then lowered by the height of one layer and the coater spreads new powder from the dispenser platform across the build platform. This process is repeated until the part is finished. The whole process takes place in a controlled atmosphere, typically argon. This is done in order to prevent contamination since the powder is entering a liquid state.

There is usually a need for support structure though the unmelted powder itself provides some support. These support structures have to be removed after the parts are finished and that can sometimes be a complicated process. The part itself also has to be removed from the build platform, typically done with a bandsaw. Further processing includes surface finishing because the surface can be too rough for curtain application. Sometimes the part also has to be machined in order to meet very fine tolerances.

2.4.2 Heat Affected Zone

As mentioned earlier the powder is fully melted and not just sintered during a Selective Laser Melting (SLM) process. Therefore, it is necessary to look a bit closer at this aspect.
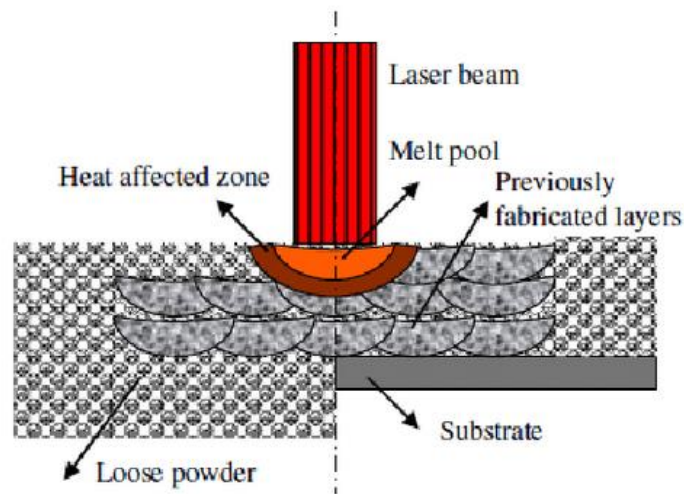

Figure 6: Cross-section of SLM process. Laser travel direction is into the picture. (Knowles et al., 2012)

In Figure 6 a cross-sectional image can be seen of an undergoing SLM process. The orange half circle indicates the melt pool, and it is along the edge of the melt pool the fusion line occurs. Further, the brown area indicates what is called the heat affected zone. This zone is affecting already solidified material, which can have a significant impact on the mechanical properties. The temperature is not high enough to melt this area, but there is sufficient heat to have some degree of impact. There could for example be a high buildup of residual stress within the material and this buildup could again lead to cracking. In order to remove the residual stress materials are often heat treated. However, some of the previous melt pool is partially melted and this can cause epitaxial grain growth to happen by allowing new solid material to form by keeping the same crystallographic of the nearby grains and the growth happens toward center of the melt pool according to maximum thermal gradient direction. Thus, the preferred growing direction being in the build direction. In previous studies it has been reported that SLM is able to produce texture and preferred crystallographic orientation of grains along the building direction. In order to prevent formation of a too intense texture in both the building and the horizontal direction a scanning pattern which rotates after every layer has been introduced. Thus, resulting in a highly isotropic structure. However, SLM manufactured parts are known to exhibit different mechanical properties in different directions due to other factors. Therefore, when it comes to 3D printing this is well known and is something one has to think of when deciding how to print a part. (Shifeng et al., 2014)

2.4.3 Advantages and drawbacks of SLM

Here are some of the advantages and drawbacks of SLM compared to traditional manufacturing methods.

Advantages:

- Produces parts with very good mechanical properties compared to other methods
- Wide range of metal materials to choose from
- Very complex structures can be realized as a result of a layer-by-layer method, which would otherwise be extremely complicated or expensive if not impossible
- Produce parts with high tolerances
- Can produce multiple parts at once
- As little material as possible is used, close to no waste material

Drawbacks:

- Expensive compared to other 3D printing technologies
- Requires very high powder quality
- Time and energy consuming
- Rough surface finish
- May require a lot of post-processing
- The size of the parts is limited

Through re-designing parts by the use of software the weight of parts can be greatly reduced. A reduction in weight does not only mean that less material is used, but a weight reduced part can also lead to a reduction in energy consumption if the part for example is going to be used in the transportation sector. This effect was studied by (Priarone et al., 2018) which showed that the effect can be quite significant.

2.5 Atomizing

There are many methods when it comes to producing suitable powder for AM. One way is by atomizing, which can further be divided into three groups as seen in Figure 7.
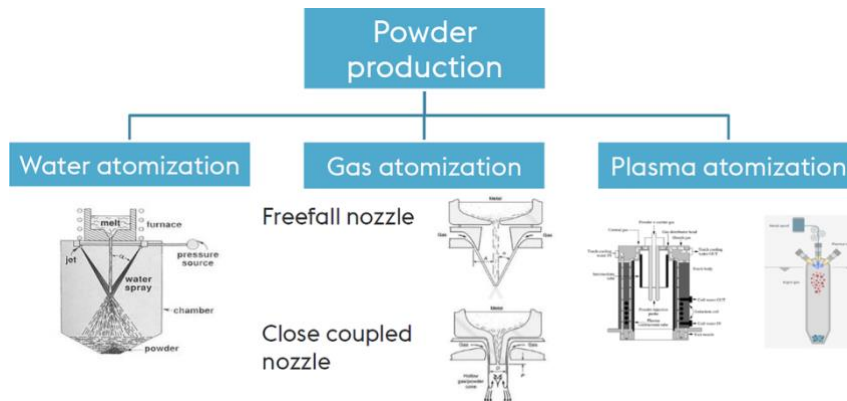

Figure 7: Atomizing methods for producing metal powder. (Wallner, 2019)

Which process that is used depends on the desired powder properties, material and cost. For example, water atomization can produce the highest volume of powder at a very low cost, but as of now the powder is not yet suitable for SLM. Plasma atomizing can produce powder with excellent powder qualities with regards to 3D-printing and can produce powder from materials with very high melting points but require that the raw material have a high quality with a certain shape (bar or wire) and the process is also very costly. The third process is gas atomization which is sort of a middle ground of the three with respect to powder quality and cost and happens to be very suitable to produce 316L powder when combined with a Vacuum Induction Melting (VIM) furnace, as has been mentioned earlier. This process is then called Vacuum Induction Gas Atomization (VIGA) and is the one used to produce the powder for this thesis; it is therefore relevant to take a closer look at this process.

2.5.1 Gas Atomizing

First, what is Gas Atomizing precisely? Gas atomizing is the use of gas to split a molten stream into fine particles. This is a very efficient method when the desired powder properties are very fine spherical particles. This process can again be divided into freefall and close coupled nozzles with the main difference being where the gas and molten stream intersects, as can be seen in Figure 8.
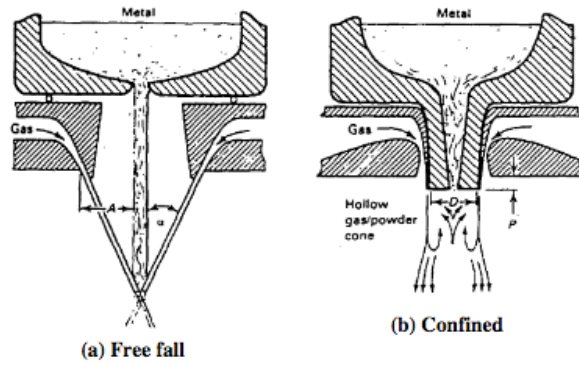
Figure 8: (a) Free fall nozzle and (b) close coupled nozzle. (Wang & Chen, n.d.)

The main advantage of the free fall system is that the nozzle is not at risk of freezing-off at the tip compared with close coupled where this can be a problem. The free fall system is also easier to operate, however it is not suitable for fine powder production due to lower efficiency (Wang & Chen, n.d.). On the other side a close coupled system is suitable to produce fine powder due to higher efficiency because the proximity of the gas and melt stream favor energy transfer (Urionabarrenetxea et al., 2021). As mentioned earlier this process can then be combined with a Vacuum Induction Melting (VIM) furnace.

2.5.2 Vacuum Induction Gas Atomization

The reason for combining these two processes can be seen in Figure 8 where an open melting chamber can be seen. An open melting chamber is the normal setup, but when wanting to produce powder from material that is highly receptive to contaminations, especially oxygen, another setup is needed. This new setup is simply constructed by replacing the open furnace with a VIM furnace. The VIM furnace provides a melting atmosphere free of contaminants by creating a vacuum before the melting process starts. After the material is melted the chemistry can be checked and new material can be added in order to achieve
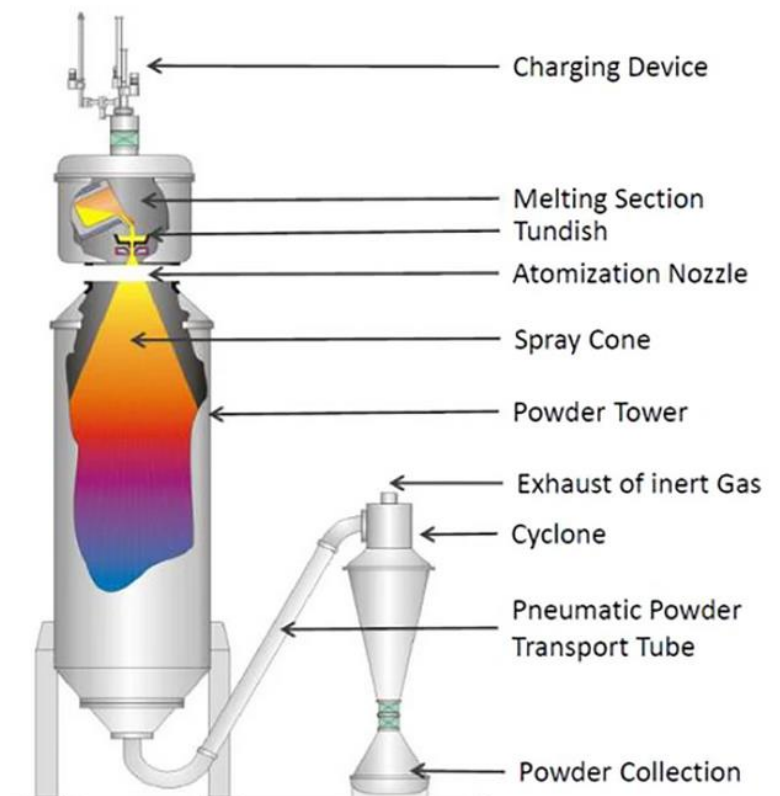

Figure 9: Schematics of Ald VIGA technology. (Wallner, 2019)

the desired composition. Before the molten material is poured into the gas atomizer the whole

atomizing system is flooded with an inert gas. Then the molten material is poured continually into the tundish system. As soon as the molten stream exits the nozzle it is disrupted by a stream of high-speed inert gas. What then happens is that there is a transfer of kinetic energy from the high-speed gas to the molten stream, which in turn becomes unstable. Then there is a dramatic pressure drop caused by the gas expanding resulting in the melt being split into droplets. The droplets are then in a free-falling state in the powder tower and because of gravity the droplets form into spheres as they solidify during the fall. Then the powder is collected at the bottom and sent through further processing where suitable droplets are extracted depending on what the powder is to be used for. Powder, especially for SLM, may need sieving in order to obtain a suitable PSD.

As can be imagined there are many variables to consider when producing powder by gas atomization. It all depends on what powder characteristics that are desired. Also, it is not so that every alloy behaves the same way either and therefore the same settings cannot be used on different alloys in order to achieve the same powder characteristics.

Some of the variables to consider are:
- Nozzle outlet diameter
- The flow rate of the material at nozzle outlet
- Flow rate of the atomization gas at the nozzle outlet
- Temperature of the atomization gas

From the time of the invention of gas atomization there have been several studies conducted on the technology in order to find optimal operating conditions. In these studies, there have been several attempts to link the median particle size of a powder (D50) with the atomization conditions through empirical correlations. A study done by (Urionabarrenetxea et al., 2021) found that a dimensionless equation proposed by Kishidaka was the most reliable equation to predict the median particle size of the powders produced in their work.

2.6 Equipment and methods
There is a large variety of tools and equipment that can be used when assessing the microstructure and measuring mechanical properties. The equipment used in this study will be further described below.

2.6.1 Light Optical Microscope

A light optical microscope utilizes visible light which is sent through several lenses in order to obtain a magnified image of an object. When working with metals the microscope is used in a reflective manner. Which means that the light is reflected by the surface of the object. Then, in order to obtain usable images, the surface must be in a mirror like condition in order to reflect as much light as possible. This is usually achieved through several steps of polishing. After polishing it is usually possible to spot any cracks or pits if they should exist, but it is also often desirable to look at the characteristics of the grains, different phases and in the case of 3D-printing, fusion lines. This is not usually visible after just polishing, but a surface where these things can be studied can be achieved through proper etching. Etching utilizes the fact that different chemical composition and high energy grain boundaries corrode at different rates dividing the surface into areas. Then, through the difference in characteristics of the areas, different amounts of light are reflected, revealing contrasts which can be studied.

Since the microscope is using visible light a camera is often used to obtain images. These images can further be analyzed by a program in order to for example determine the percentage of different phases or percentage of cracks and pits at the surface. It has to be said that though a light optical microscope can obtain very high magnifications compared to what the naked eye can see. It is limited by the wavelengths of visible light, resulting in the maximum magnification being in the range of 500x to 1500x(*Limitations of Optical Microscopy*, 2017). Therefore, if a higher magnification is needed an electron microscope may be used. Nonetheless it is not really the magnification that matters, but it's the resolution that matters and an electron microscope does usually have a better resolution.

2.6.2 Hardness measurement

Hardness testing is a method used to measure the property of the material to withstand plastic deformation on physical impact. A hardness value is not a fundamental property, but factors such as load on the indenter, load duration and the indenter geometry have to be taken into consideration when evaluating the value. The value itself is unitless and can be expressed by the equation below. Where P is the loading and d is the mean value of both diameters.

$$HV = 1.854\frac{P}{d^2}$$

The Vickers hardness test is suitable for a wide range of materials and can in fact be used for all metals. This hardness test is also considered easier to use than others because the size of the indenter does not affect the calculations and the indenter itself can be used for all materials. The calculated value is expressed by the equation above, which in fact is called Vickers Pyramid Number. The only fixed specification for the Vickers hardness test is the geometry of the indenter which has to be in accordance with ISO 6507-2 or ASTM E384. Other factors such as load, and duration has to be chosen according to the standards. Another factor to consider is the spacing of indentions which has to be done in accordance with for example ISO 6507-2 section 8.8.

2.6.3 Tensile testing

Tensile testing is a method where a test piece is extended until fracture. This is done in order to find the Young modulus, yield strength, tensile strength, maximum elongation and reduction of area of a material. This sort of testing will also reveal if the material is ductile or brittle, but tensile strength is not usually important in very ductile materials. However, it is very important in brittle materials and tensile testing is very important in determining how the material will behave. Tensile properties also give a strong indication on how the microstructure might be.

There are many ways to do tensile testing, but certain criteria must be met. First of all, the machine being used must be certified according to ISO 6892-1, ASTM E8/E8M or equivalent. Thereafter the specimen should have a dog bone shape. The reason for this is to control where the fracture will occur in order to get proper results and measure the elongation. As mentioned, the specimen should have a dog bone shape, which means that the ends will have larger diameters than the midsection. Further in the case of round specimens one is free to choose the two different diameters as long as the ratio between the two diameters are in accordance with a relevant standard. When diameters are chosen the standard specifies how the transition radius between the two different diameters must be. When it comes to length, the ends can be as long as possible since this is the gripping area, but the midsection must be in relation to the diameter. In ASTM E8/E8M one can find suggested specimens with dimensions that follow all the criteria of the standard. In order to get proper results at least three specimens must be tested of the same material.

2.6.4 Impact testing

Impact testing tests a material's ability to withstand a sudden and concentrated impact. The most used form of impact testing is the Charpy V-notch test which determines how much energy the material can absorb during fracture. A Charpy test has to be done on a machine that is certified in accordance with a relevant standard. The specimens being used should be 50 mm long and the cross section should be 10 by 10 according to ISO 148-1:2016. If this cannot be met there are exceptions, but deviation from those dimensions is not desirable. Further there has to be a v-notch or u-notch in the middle of the specimen, which is also specified in the standard. An impact test is conducted by releasing a mounted sledgehammer from a raised position, which

Figure 10: Impact testing machine.

swings and hits the specimen at the bottom of the curve. The amount of energy that was absorbed can then be read of a measuring device. It is usually measured in joules.

3 Powder and samples

3.1 The powder

The "green" powder used to produce the samples was produced by RINA Consulting CSM. They used Vacuum Induction Gas Atomizing (VIGA) to produce the powder. This is as talked about in the literature study a very suitable process to use when producing stainless steel powder for L-PBF. The raw material, also referred to as scrap material which can be seen in Figure 11, were unused parts from storage. These parts were passed through a cleaning process though the parts were fairly clean, but this was done in order to imitate the use of used parts as raw material. The scrap material used accounts for about 90% of the raw material used. The other 10% is new material that has been added in order to obtain the chemistry of 316L, particularly nickel had to be added. The entire batch of a 100kg required 15 single atomizing processes, because of the small sized system RINA is running.

Figure 11: Some of the scrap material used in the atomizing process.
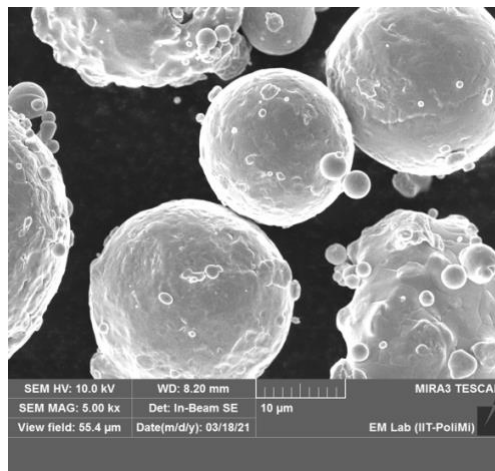
Figure 12: SEM image of 316L "green" powder.

The powder distribution is presented in Table 2. D5 and D10 refers to 5 and 10 percent of the powder being finer than the respective micrometers. D90 and D95 refers to 10 and 5 percent being coarser than the respective micrometers. D50 refers to the middle of the distribution.

Table 2: The particle size distribution of the powder that was used to produce the samples.

PSD	RANGE	D5	D10	D50	D90	D95
µm	20-63	18.50	20.90	34.30	55.20	61.50

3.2 The samples

The samples studied were provided by Aidro. They used an EOS M290 single laser machine to create the samples. This machine is a metal 3D printer with selective laser melting technology and the powder used was the "green" powder produced by RINA. The machine used an energy density of 58 J/mm^3 and the layer thickness was set to 40 µm a layer. The laser scanning direction rotated about 50º after each layer. The number of specimens provided is in accordance with DNVGL-ST-B203 and a 3D model of the samples can be seen in Figure 13. None of the samples were heat treated after printing.
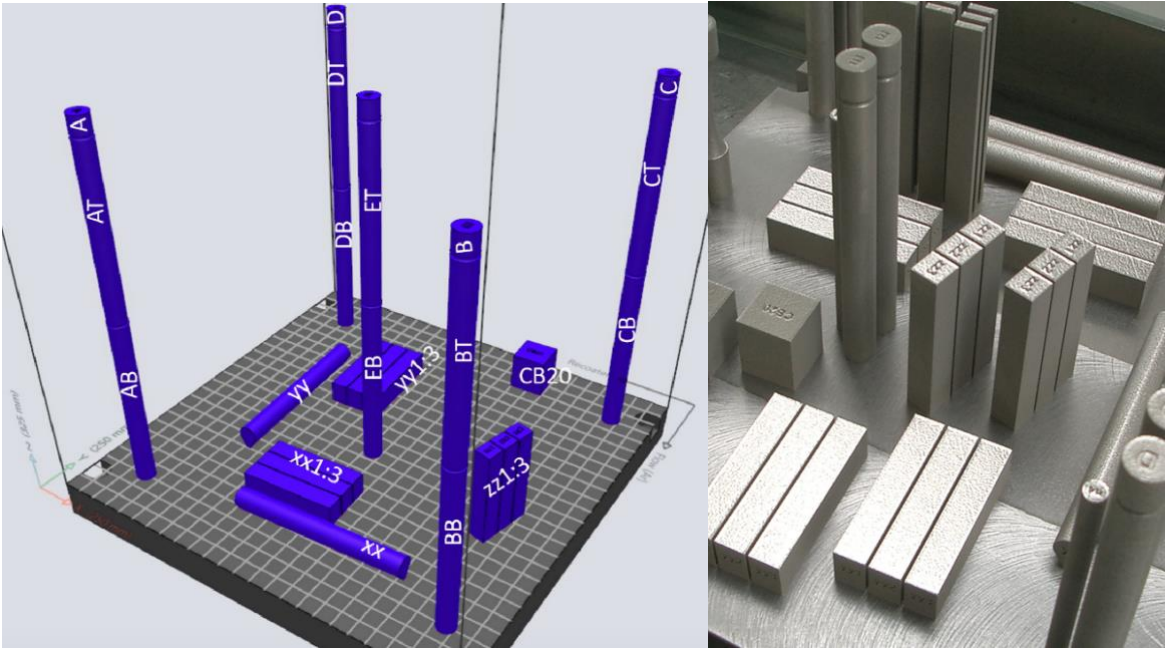
Figure 13: To the right: 3D model of the samples provided. To the left: The finished samples.

In total there are 17 specimens. This includes seven tensile specimens (only the non-elevated), nine impact specimens and one cube. The cube can be seen in Figure 13 as CB20 and has dimensions of 20x20x20 mm and was used for microstructural analyses. The tensile specimens are according to ASTM E8 Figure 8 specimen 3 and the impact specimens are also according to standard with the standard dimensions of 55x10x10.

Table 3: The tensile and impact specimens listed according to print direction and original name in 3D model.

	TENSILE	**IMPACT**
X-DIRECTION	XX	XX1-XX2-XX3
Y-DIRECTION	YY	YY1-YY2-YY3
Z-DIRECTION	A(AB), B(BB), C(CB), D(DB), E(EB)	ZZ1-ZZ2-ZZ3

4 Experimental procedures

4.1 Sample preparation
In order for the different tests to be properly carried out the specimens needed some preparation. The impact specimens did not need much work, but the tensile specimens did. For the microstructural, hardness and porosity assessment the cube was used. In order to get a good picture of the structure in different directions samples had to be tactically extracted. Preparation of the different samples will be further described below. None of the specimens were heat treated.

4.1.1 Tensile specimen preparation
In Figure 14 it can be seen that the cross section of the tensile specimens was uniform. As mentioned earlier, uniform tensile specimens are not very well suited for testing since it is uncertain where the fracture will occur. Therefore, these specimens had to be machined, which was done by the help of Computer Numerical Control (CNC) in order to satisfy the standard. Before they could be machined by CNC the XX and YY samples had to be machined in order to obtain a circular cross section, which they did not originally have because of support structure. This was done manually and without any cooling. The diameter was approximately the same after machining as before. Then the top of the Z oriented specimens, which can be seen in Figure 14, had to be cut off. This was accomplished with Struers Discotom-5 and this machine uses large amounts of coolant in order to avoid any heating and so does the CNC machine. After this the specimens were handed over to an operator which did the CNC machining.

Figure 14: Finished tensile specimen.
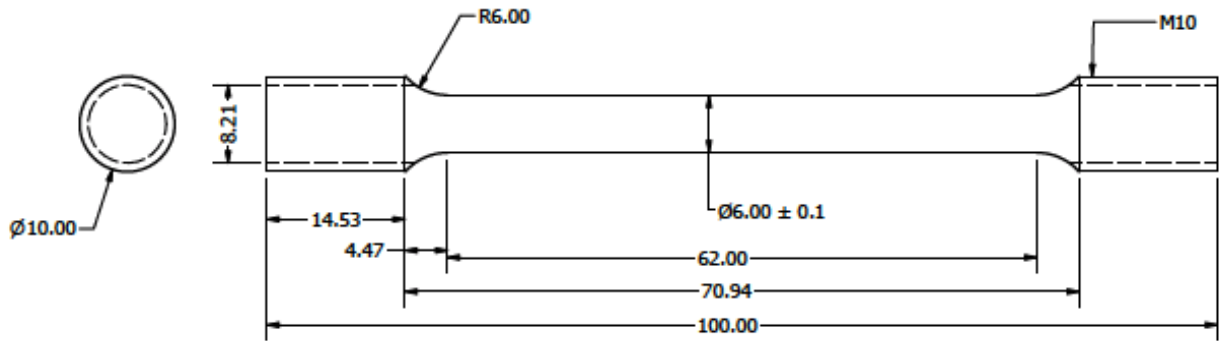
Figure 15: Machine drawing with dimensions (mm) of the tensile specimen.

As can be seen in the drawing, the gauge length is longer than the specified gauge length in ASTM E8, but the standard allows for a longer gauge length in order to accommodate an extensometer.

4.1.2 Impact specimen preparation

The dimensions of the impact specimens were all within the standard and therefore these specimens only had to get the v-notch made, as can be seen in Figure 16. The v-notches were also made by the help of CNC, where a sufficient amount of coolant is used. DNVGL-ST-B203 states that for x- and y-oriented test specimens the notch shall be orientated parallel to the build direction. This was accomplished by placing the notch on the same side of all of the specimens. Regarding the z-oriented specimens it did not matter which side the notch was on, but nonetheless the the notch was placed on the same side of all the specimens.
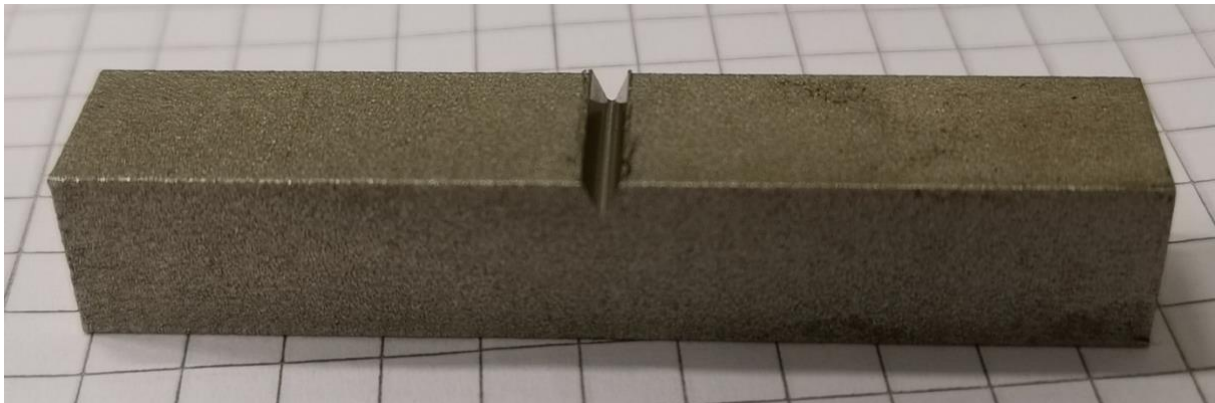
Figure 16: Finished impact specimen.

4.1.3 Preparation of the cube

Since the cube was not to undergo any destructive testing, it was very well suited for microstructural analysis. After some examination it was decided to get one sample from the top and one sample from each of the sides perpendicular to each other. The cutting was carried out with Struers Discotom-5 which uses a sufficient amount of coolant.
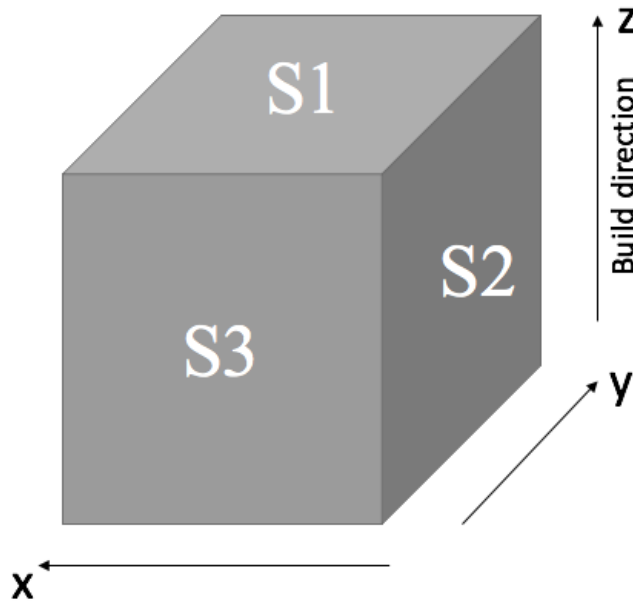
Figure 17: Image of the cube and where the samples are taken from.

As can be seen in Figure 17, the sample from the top is named S1. The sample from the yz-plane is named S2 and the sample from the xz-plane is named S3. For the sake of clarity, the x- and y-oriented specimens the notches are cut directly into the xz-plane and yz-plane respectively.

4.2 Microstructural analysis

When the cutting was finished the samples needed further preparations since cut surfaces are not suitable to analyze. This is because any pores or cracks may have been evened out during cutting. As talked about earlier, in order to be able to analyze the samples with the light optical microscope the surface of the sample needs to be in mirror-like conditions. Which can be achieved through grinding and polishing. The samples were also going to be etched in order to expose fusion lines and grain boundaries. Therefore, it was necessary to use ConduFast, which is conductive, when casting the samples. When etching it is important that the current goes through the samples, therefore ClaroFast was used as a nonconductive casting material that covered almost all of the sample.

4.2.1 Specimen preparation for Light Optical Microscope

Before any analysis with a light optical microscope could be carried out the samples needed some preparation. The samples were first thoroughly cleaned before they were cast using Struers Citopress-30. When the samples were cast most of the sample itself were covered in ClaroFast, as can be seen in Figure 18. Then when ConduFast was added it was important to

make sure that it had sufficient contact with the sample. When looking closely at Figure 18 it is possible to see the ConduFast and that the sample is sort of planted in it. The samples were casted in order to reduce any error from handling the samples during grinding and polishing and to make the etching possible. In Figure 18 a sample E can also be seen, and this sample is the top of tensile specimen E that had to be cut off. Sample E was only used for porosity assessment.
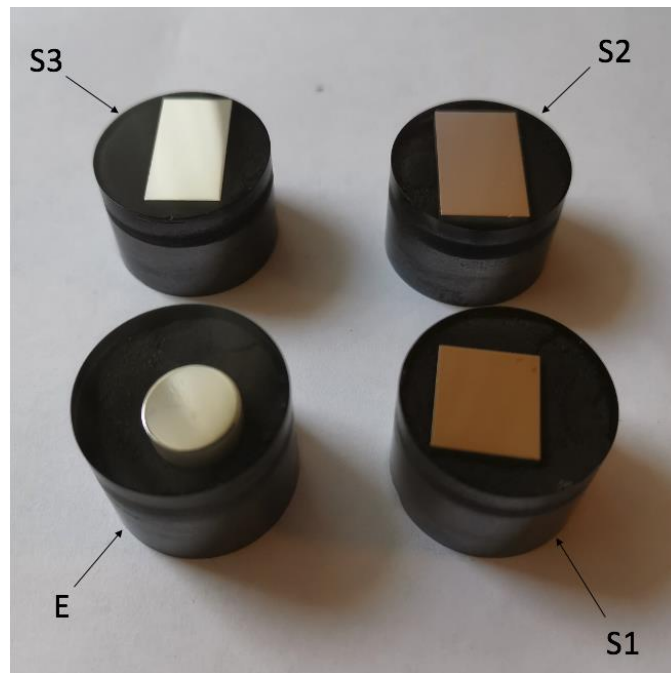

Figure 18: Sample 1-3 and E, casted in ClaroFast and ConduFast.

The grinding and polishing were carried out on a Struers Tegraforce-5. The carried-out procedure is a 6-step procedure and was created by an earlier master student. The reason for following this specific procedure is because the procedure was made for 316L and it exhibited very good results. The procedure is also in accordance with ASTM E03. Between each step the samples were thoroughly cleansed by Struers Lavamin and the entire procedure can be seen in Table 4.

In order to reveal specific parts of the microstructure the samples were etched. The etching was conducted by the use of Struers Lectropol-5. The etching procedure followed was also created by an earlier master student which also obtained good results when etching 316L. The proposed procedure was to etch the samples with 10% aqueous oxalic for 24 seconds with 15V applied. The first sample that underwent the etching was S2 and because the etching was quite effective the process was stopped after 20 seconds. Then sample S1 were etched for 20 seconds, which could seem a bit long and therefore the last sample S3 was etched for 15 seconds. The voltage was kept at 15V for all three samples.

The samples were then analyzed with an Olympus GX53 and several micrographs were taken of the microstructure and various magnifications. The etching was quite successful, and there was therefore no need to redo the process. An integrated software called Olympus Stream was used to analyze the microstructure. Further, this program has a function called phase analysis and this was used to analyze the porosity. The phase analysis was carried out by taking an image of the surface and then using the program to estimate the porosity. Several images were taken across the surface of each sample with 50x magnification as suggested by DNVGL-ST-B203 in order to get a good overall picture of the porosity. This magnification resulted in the examination area of each image being approximately 0.04865 mm^2.

Table 4: The grinding and polishing procedure.

STEP	GRINDING AND POLISHING	LUBRICANT	TIME
1	Piano 220 µm	Water	2 m 00 s
2	Piano 600 µm	Water	2 m 00 s
3	Piano 1200 µm	Water	3 m 00 s
4	Allegro	Allegro/Largo 9 µm	3 m 00 s
5	Dac	Dac 3 µm	6 m 00 s
6	Mol	Nap B 1 µm	8 m 00 s

4.2.2 Hardness examination

The hardness was assessed on a NOVA 330 using HV/10 test method, as proposed by the DNVGL-ST-B203. The load was therefore 10 kg and the dwell time for the indentation was set to 10 seconds. The testing was performed on sample S1, S2 and S3. Before the hardness testing could be carried out the samples had to be grinded and polished once more in order to remove the effect of the etching, but only step 4 through 6 was necessary to carry out. The testing itself has been carried out in accordance with ISO 6507-2 and indentation has therefore been performed within the frame of section 8.8. The indentations were taken across the longest side of the samples in order to get as many indentations as possible. The first and last indentations are more than 2 mm from the edge of the sample and the distance between the center of each indentation is 1.5 mm. This is about 5 times the diameter of the indentations. The reason for the chosen distance is because 316L is a soft material and in order to be sure to get proper results this distance was chosen. There were taken a total of 26 indentations, six on S1, nine on S2 and eleven on S3.

4.3 Tensile testing

The tensile testing was carried-out in accordance with ASTM E8 except for one deviation from the standard which was discovered after testing. The deviation was the placement of an extensometer, but this deviation has only affected the elongation results. Before testing started the specimens were inspected for any cracks or irregularities and the diameter and gauge length was measured as well. The diameter of each specimen was measured in at least three places and they were all within the standard. Then the machine was made ready for testing. The speed of testing was set to 0.015 mm/mm/min up until 0.2% when the yield strength was recorded, after that the machine was set to increase the speed to 0.1 mm/mm/min and maintain it until fracture.
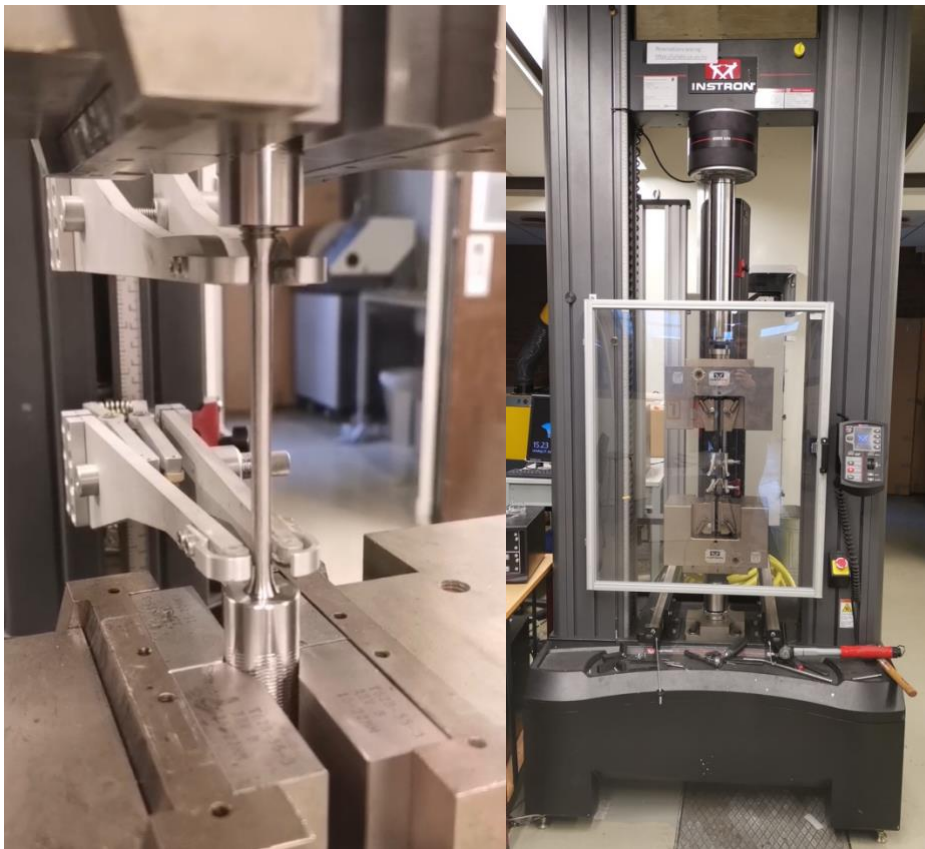
Figure 19: The machine and a specimen placed in the machine with the extensometer in place.

The extensometer was set to a gauge length of 55 mm, which is the length between the two arms seen in Figure 19. This was done in order to capture as much of the extension as possible. After fracture the reduced area was calculated for each sample. The testing was carried out at room temperature.

4.4 Impact testing

The impact testing was carried out in accordance with ISO 148-1:2016 at room temperature. The measurements of every specimen were recorded before testing. The notch was as mentioned placed parallel to the build direction as instructed by DNVGL-ST-B203. When placing the specimen, it is important that the notch is facing away from where the hammer is going to hit. It is also important to make sure that the specimen is centered and in order to accomplish that a special set of pliers is used as described in the standard. In addition to making sure the specimen is centered it is also important to make sure that there is no room between the specimen and the support structure since this can cause irregularities in the results. If the specimen after impact should not break it is important to take a note of that.

5 The results

5.1 Tensile results

The results from the tensile testing are presented in Table 5 and as it can be seen exhibited the YY specimen the highest yield strength, ultimate tensile strength and E-modulus. While the z-oriented specimens exhibited the greatest elongation and reduction of area, which also can be seen in Figure 20. However, the yield and tensile strength are significantly lower in the z-direction compared with the other two directions. It can also be reported that every specimen fractured and there was no slippage in the grips.

Table 5: The results from tensile testing. YS – Yield Strength, UTS – Tensile Strength, EL, Elongation, RA – Reduction of Area, E – E-modulus/Young's modulus and SD – Standard Deviation

ORIENTATION	SPECIMEN NAME	YS 0.2% (MPA)	UTS (MPA)	EL (%)	RA (%)	E (GPA)
X	XX	519.3	619.1	31.2	62.4	110
Y	YY	541.9	631.1	33.1	62.1	134
Z	Average	455.8	554.2	38.5	63.5	104
	SD	2.45	6.34	0.74	1.25	5.59

5.1.1 Strain vs Stress

All seven stress and strain curves of the tensile samples are presented in Figure 20. The area under each curve has also been calculated and the lowest area is to be found under the curve of specimen XX, which is distinctively lower than the others. The area under specimen YY and the z-oriented specimens are quite close in sizes, but on average the area of the z-oriented specimens is slightly smaller.
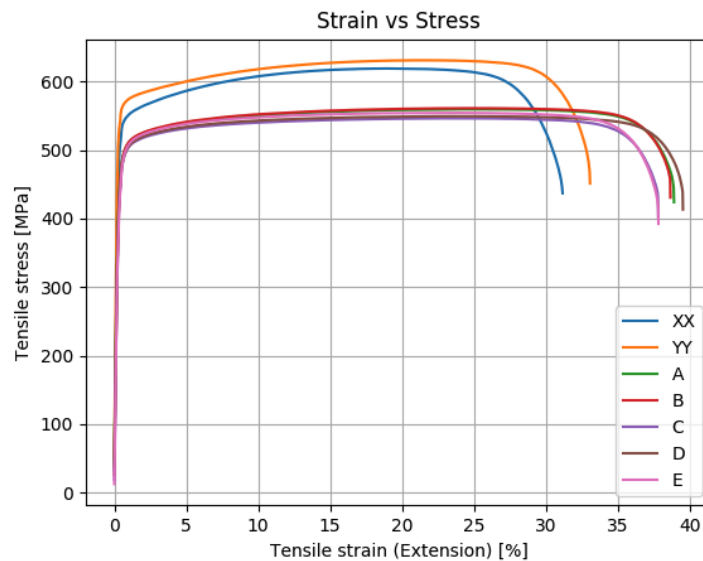
Figure 20: Strain vs Stress curves of all samples.

5.2 Impact results

The results from the impact results are presented in Table 6. As it can be seen exhibited the x-oriented specimens the greatest impact toughness, followed by the y-oriented specimens and then the z-oriented specimens. The x- and y-oriented specimens seem to exhibit very consistent values in their respective directions compared to the z-oriented specimens which seems to exhibit slightly inconsistent values. However, it can be reported that every specimen completely broke.

Table 6: The results from impact testing. Everything is in Joules.

ORIENTATION	AVERAGE	MAX	MIN	SD
X	99.6	101.6	98.3	1.4
Y	82.7	84.2	80.6	1.5
Z	71.2	76.4	67.4	3.8

5.3 Hardness results

The results from the hardness measurement are presented in Table 7. Figure 17 is also presented for practical considerations. As the results show did sample S2 exhibit the highest hardness, followed by S1 and then S3. The hardness did also vary across the surface as shown by the max, min and standard deviation values.

Table 7: The results from hardness testing. HV/10.

Sample	Measurements	Avg	Max	Min	SD
S1	6	214.8	219.4	208.6	4.34
S2	9	222.6	234.9	216.1	6.41
S3	11	204.6	210.6	195.5	4.81
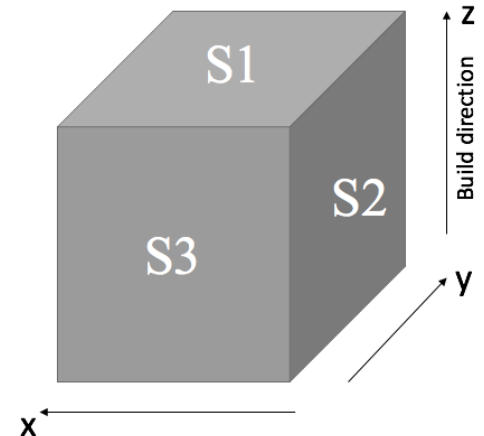
5.4 Porosity results

The results from the porosity assessment are presented in Table 8.

As mentioned earlier was a magnification of 50x used which resulted in the exanimated area of each image being approximately 0.04865 mm^2. When examining the samples some pores and cracks where seen where some of them were quite significant, hence the max value of specimen S1 and E. Which are also quite similar due to the fact that they in a way are taken on the same surface, but just on different specimens from different elevations within the build chamber. All in all, few pores and cracks were observed, hence the average values.

Table 8: The results from porosity assessment given in percentage.

Sample	Number of images	Avg	Max	Min	SD
S1	12	0.36	1.53	0.03	0.48
S2	10	0.17	0.43	0.07	0.12
S3	12	0.29	0.79	0.04	0.25
E	12	0.37	1.24	0.04	0.37

5.5 Images from the light optical analysis

The first image that can be seen in Figure 21 is taken of the top of the cube (S1). The second image can be seen in Figure 22 and is taken by the xz-plane of the cube. The last images are presented in Figures 23, 25 and 25 and are taken by the yz-plane of the cube.

5.5.1 The laser scanning pattern

Figure 21 clearly shows the different oriented layers where the laser tracks are easy to recognize as a result of etching. As of the bottom layer it seems like the laser tracks are closely packed and a very consistent width of about 95 µm can be measured. It is also possible to observe that the laser scanning direction rotates after each layer in Figure 21 by being able to see three differently oriented layers.
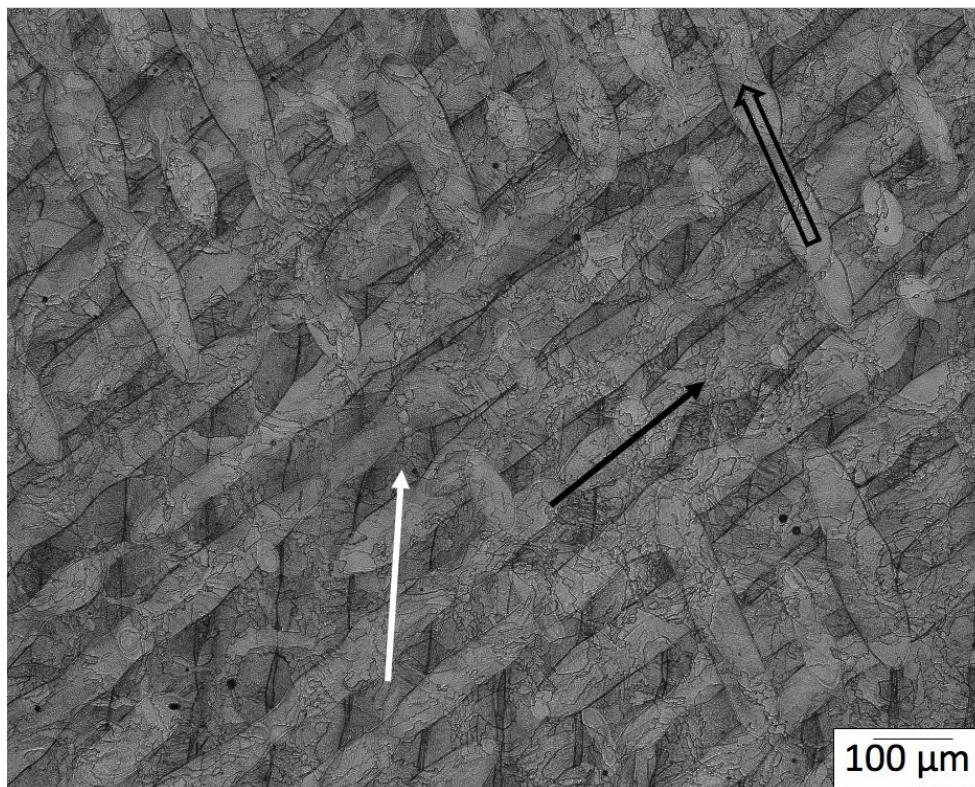
Figure 21: Image from the top (S1) at 10x. Three layers of laser tracks can be seen. The bottom layer is indicated by the white arrow, the middle layer by the black arrow and the upper layer by the open arrow.

5.5.2 Longitudinal laser tracks in the xz-plane

In Figure 22 white arrows are pointing to what is believed to be longitudinal laser tracks going in the x-direction. As mentioned earlier, the laser scanning direction rotates about 50° after each layer. This would mean that the pattern is repeated after every 18 layers or every 0.72 mm with a layer thickness of 40 μm and after measuring it seems like the longitudinal laser tracks are in fact following this repeating pattern.
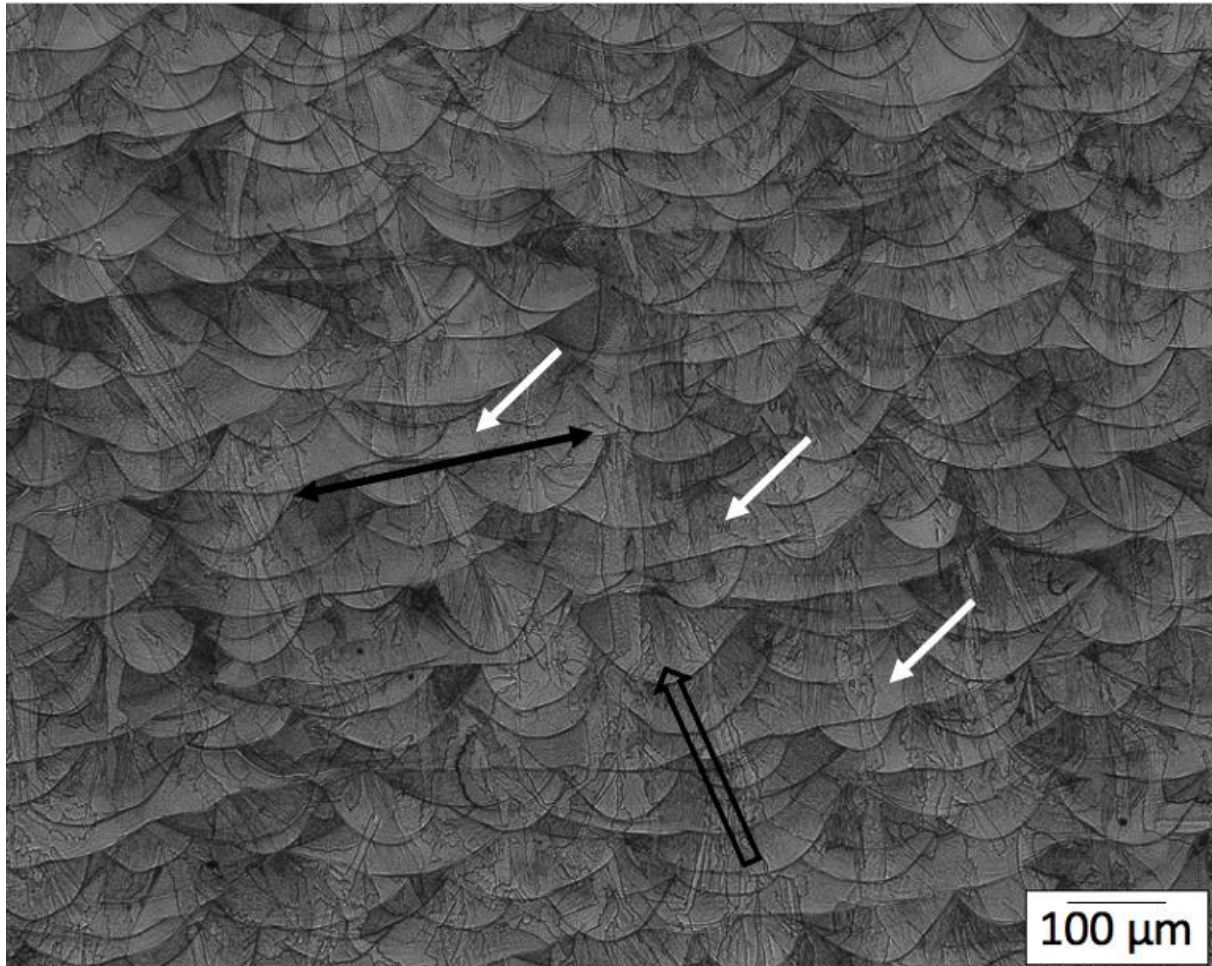
Figure 22: Image of the xz-plane. White arrows are pointing to longitudinal laser tracks, black arrow indicating the direction of the laser track and the open arrow pointing to one of many melt pools.

5.5.3 The melt pools

When looking at Figure 23 one can see that the melt pools are repeated in a very consistent pattern throughout the yz-plane, while there being no obvious longitudinal laser tracks going across the plane, only a few slightly extended melt pools. However, it is possible to see overlapping melt pools, indicated by the black arrows.
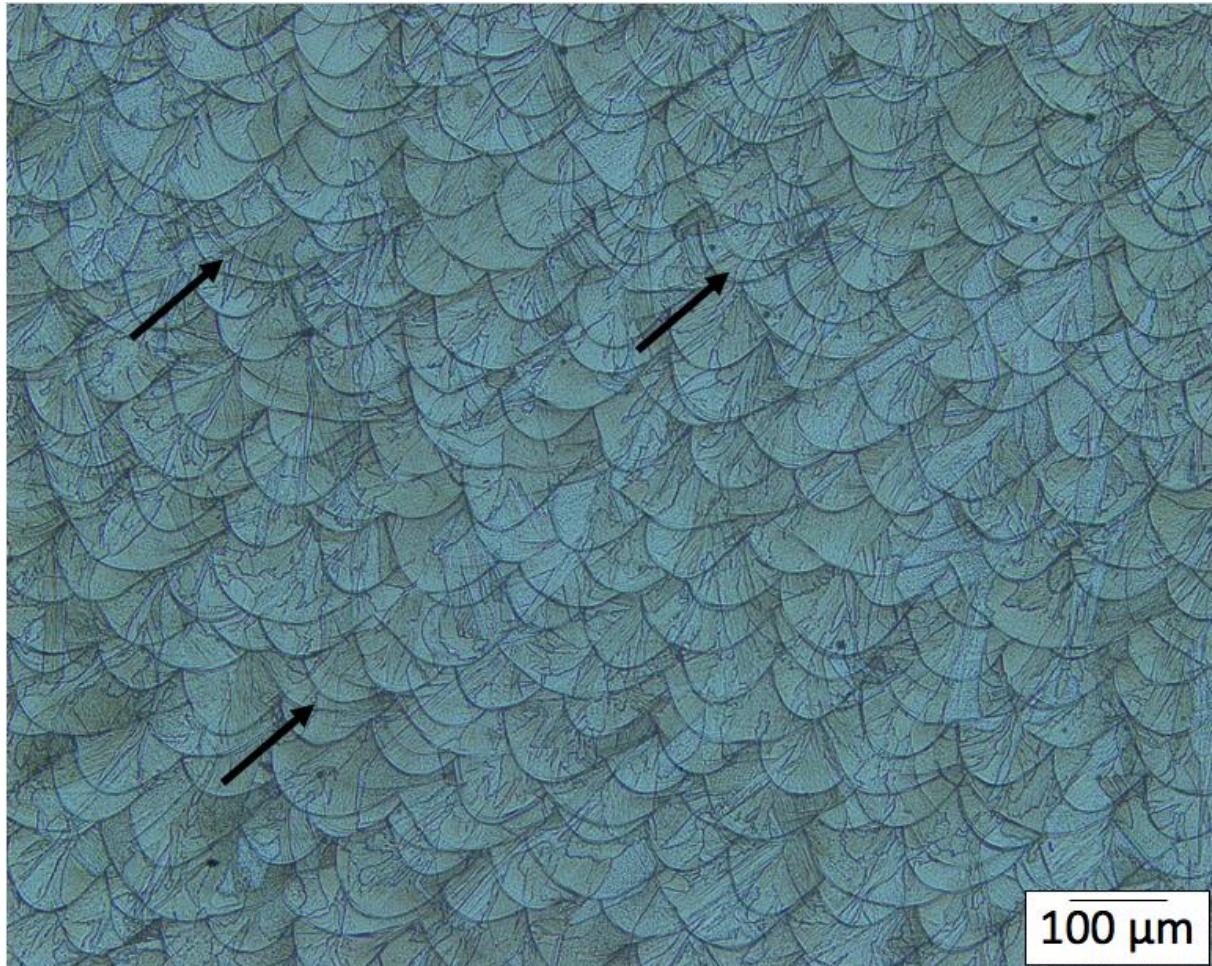
Figure 23: Image of the structure in the yz-plane (S2). The black arrows indicate overlapping melt pools.

5.5.4 Grain growth

An image of the grain structure in the yz-plane can be seen in Figure 24. In the image there can be seen grains with very different shapes and sizes stretching out in every orientation. Thus, giving the impression of there being no obviously preferred growing direction, though some of the grains can be seen crossing one or several fusion lines indicating epitaxial growth.
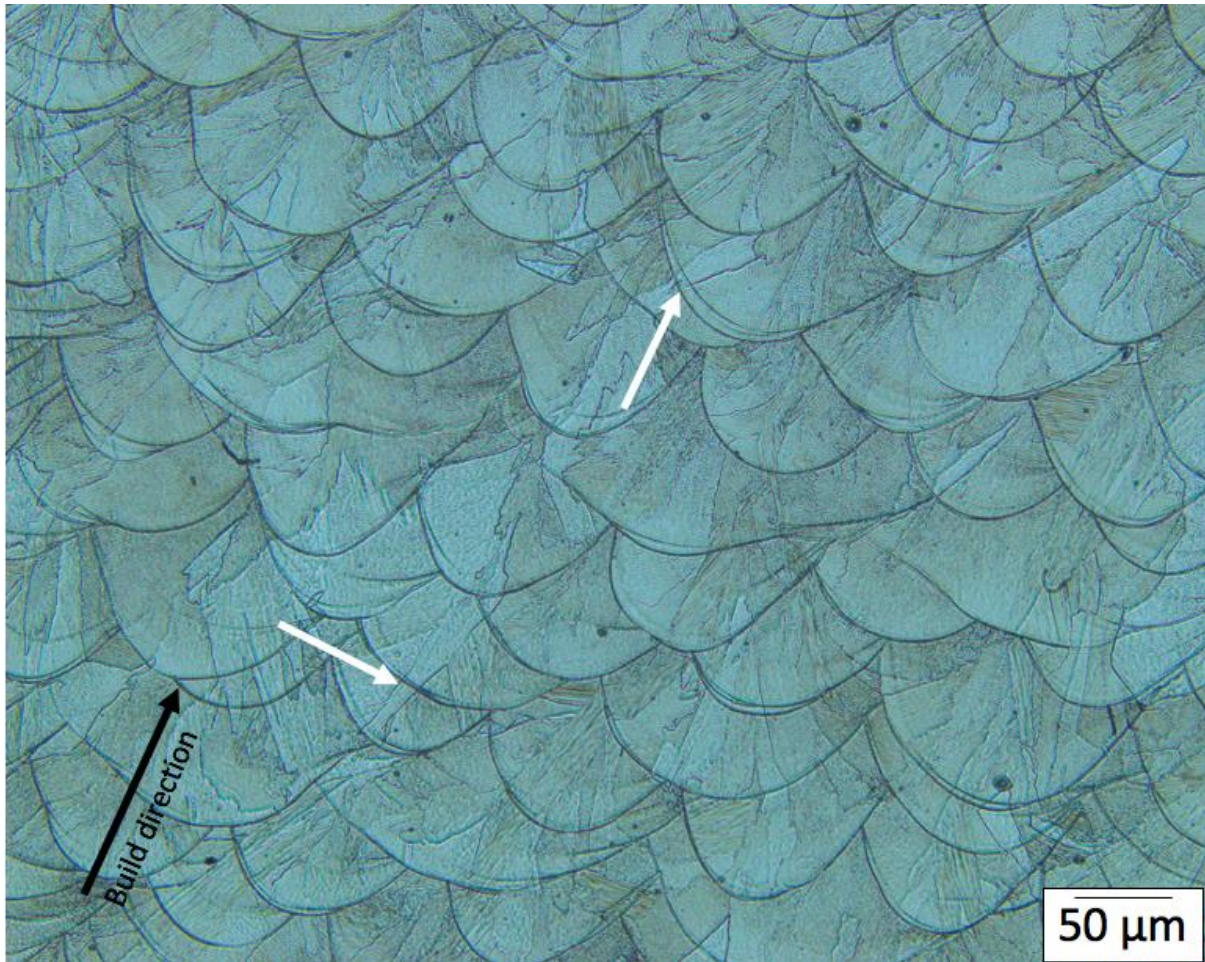
Figure 24: Grain growth in the yz-plane. White arrows indicating grain growth past the fusion line. The black arrow indicates the building direction.

5.5.5 Grain growth past the fusion line

As mentioned above, there could be seen grains crossing the fusion line and in Figure 25 such a grain is shown. This type of grain is then called a columnar grain because of its shape and is an example of epitaxial growth since it looks like it has grown in the building direction.
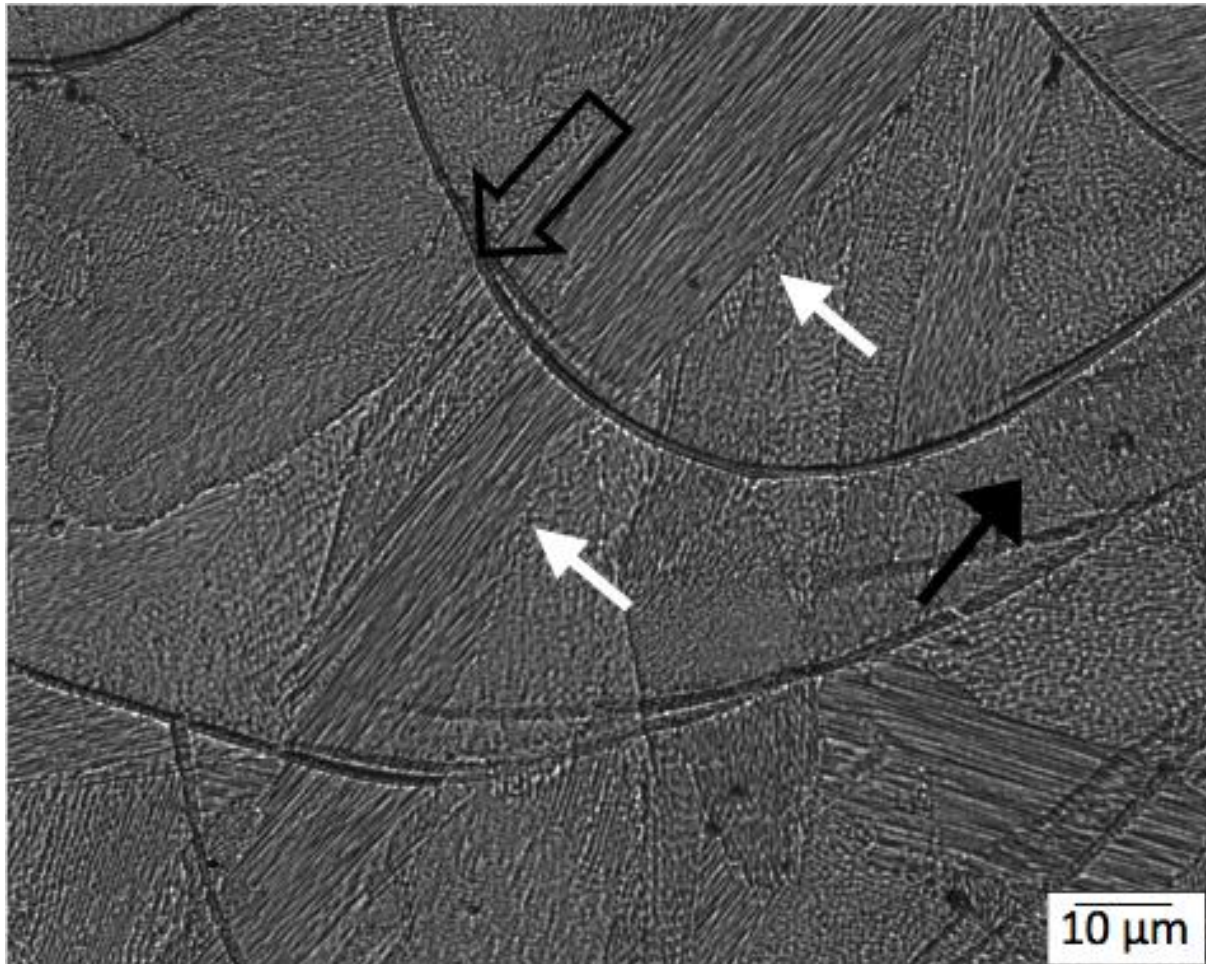
Figure 25: Image of the yz-plane (S2). The white arrows indicate example of columnar grains that cross the fusion line. Growth direction is shown with black arrows while fusion line is indicated with open arrows.

6 Discussion

6.1 Assessment of mechanical properties

As the purpose of this study is to investigate if 316L powder for Selective Laser Melting (SLM) can be made from scrap material by the process of Vacuum Induction Gas Atomizing (VIGA). A good indication of whether the powder is suitable or not is to check if the mechanical properties of the printed parts are within standard requirements. Minimum tensile requirements for additive manufactured 316L parts by powder bed fusion can be found in ASTM F3184:2016 Table 3 and is presented in Table 9. The requirements are the same for all orientations and it has to be noted that the minimum required elongation according to ASTM F3184 is measured in 50 mm or 4D (diameter).

Table 9: Minimum tensile requirements according to ASTM F3184:2016 presented with the results of this study.

	YS 0.2% (MPA)	UTS (MPA)	EL (%)	RA (%)
THIS STUDY (X)	519.3	619.1	31.2	62.4
THIS STUDY (Y)	541.9	631.1	33.1	62.1
THIS STUDY (Z)	455.8	554.2	38.5	63.5
ASTM	205	515	30	30

6.1.1 Tensile results compared with ASTM and reported results from Tec Eurolab[1]

As it can be seen in Table 9 the tensile properties of all specimens are well above what is required except for the elongation which is not fully comparable because of how it has been measured. As talked about earlier the idea was to capture as much of the extension as possible by placing the arms of the extensometer at the ends of the reduced section and thus ending up with a gauge length of 55 mm. It was only discovered afterwards that the gauge length should have been set to 4D (24 mm in this case). The reason for the discovery was because of a comparison between the results of this study and the results of testing conducted by Tec Eurolab. Which has tested specimens made from the same powder as the specimens of this study. Tec Eurolab did also used the specimens according to ASTM E8 Figure 8 specimen 3 for tensile testing. The difference is that they measured the extension in 4D, as dictated by ASTM E8 and as a result they recorded an average elongation of 49.3% in the z-direction and 38.5% for XX and 39.5% for YY. This shows that the elongation is not just within the limits, but well above the required elongation. All the other results obtained by Tec Eurolab are on the other hand very consistent with the results of this study, only very small variations. It is though

---

[1] The Tec Eurolab report can be found in Appendix C.

interesting that the elongation measured is different when it is measured over different gauge lengths. A possible explanation to the different elongation given by ASTM E8 is that of a slimness ratio, which is the relation between gauge length and cross-sectional area, where a smaller ratio would give a greater elongation. Another explanation is that the central region (24 mm) deforms more than the outer regions. Why this is the case would need more investigation.

6.1.2 Tensile results compared with the results from a master thesis[2]

In addition to the comparison with Tec Eurolab, the tensile results have also been compared to the results obtained for a master thesis, studying the microstructure and mechanical properties of 316L produced by SLM with regular powder. The samples of the master thesis were also produced by Aidro and have undergone the same machining as the samples of this study. It is also worth noting that the tensile and impact testing were performed in cooperation between the two studies in order to produce comparable results, which are presented in Table 10.

Table 10: Comparison of tensile results from this study and the master study.

ORIENTATION	POWDER	YS 0.2% (MPA)	UTS (MPA)	EL (%)	RA (%)
X	This study	519.3	619.1	31.2	62.4
X	Master study	558.9	663.0	29.1	-----
Y	This study	541.9	631.1	33.1	62.1
Y	Master study	582.2	674.7	29.1	-----
Z	This study	455.8	554.2	38.5	63.5
Z	Master study	488.2	581.9	30.8	-----

As can be seen in Table 10 the tensile specimens of this study perform very similar to the specimens of the master study. Though both the yield and ultimate tensile strength is overall higher for the master study there is less elongation, which was measured in the same way. For both studies there can be seen a difference in the measured properties in the x- and y-directions. In regard to this study the difference can be viewed as a positive sign because it indicates that the "green" powder has produced specimens with similar behavior as the regular powder, but the difference itself between XX and YY will be addressed later. Exactly why there is a difference in the mechanical properties of the two studies one could only speculate that it has to do with the chemical composition, which due to circumstances could not be tested. However, it has been told by Aidro in a private call that the "green" powder did not have the same

---

[2] This master study has been conducted by Shusil Bista at the University of Stavanger in the spring of 2021.

chemical composition as the regular powder before printing and thus strengthening the theory of the specimens also having different composition after printing. Though this may not be the entire reason for the difference and therefore further investigation is needed in order to give a complete explanation.

6.1.3 Difference in x- and y-direction

When looking at the difference in x- and y-direction it is also relevant to bring in the results from impact testing where there is also a difference, but just the opposite. Technically, before testing one could imagine that the results in x- and y-directions would be more or less the same, but as of the results this is not the case. A possible explanation could be that the difference is caused by the printing pattern. Which as mentioned earlier works by rotating the laser scanning direction about 50º after each layer. This would mean that the pattern is repeated after every 18 layers. Which is a very rapid rotation compared to a 67º rotating pattern which repeats every 180 layers, but not as rapid as a pattern rotating 90º (every other), which would actually exhibit samples in x- and y-direction with almost identical results. It has to be said that a 50º rotation is used in order to achieve close to isotropic properties especially in regard to the z-direction. That said, it is therefore conceivable that because of the number of layers it takes to make one rotation the structure of specimen XX is slightly different from the structure of specimen YY. This theory is further strengthened by the light optical images of the xz- and yz-planes.
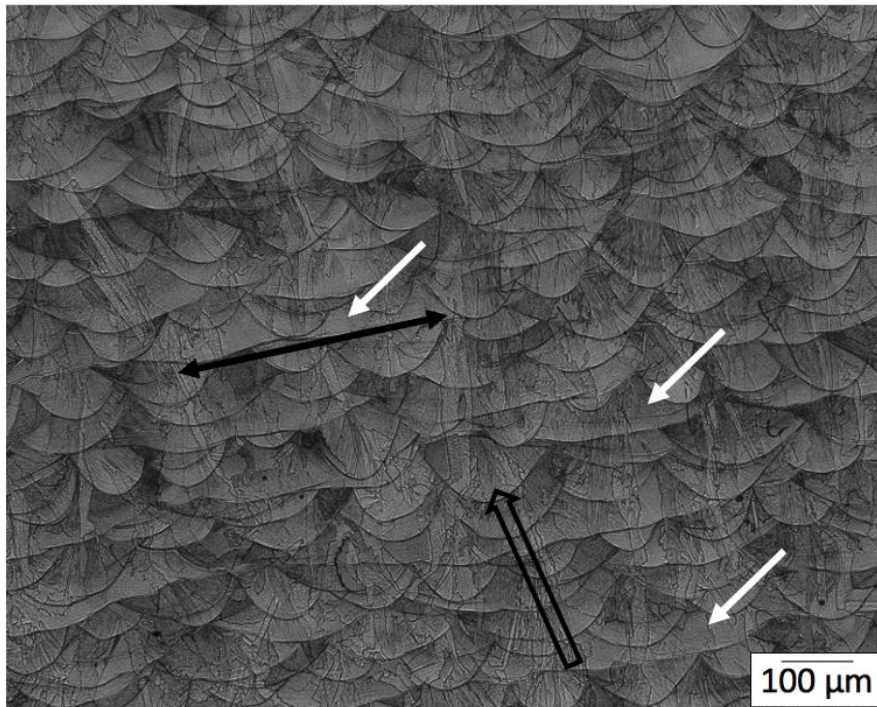
Figure 26: Image of the xz-plane. White arrows are pointing to longitudinal laser tracks, black arrow indicating the direction of the laser track and the open arrow pointing to one of many melt pools.

Just by looking at Figure 26 and 27 one could make the argument that the structure in the two planes is not the same. This is of course by assuming that the structure seen in the two figures is representative of the structure found throughout the sample (CB20) and in every other sample. That said, probably the most notable difference is what is believed to be longitudinal laser tracks going in the x-direction, pointed out in Figure 26 (xz-plane) by white arrows. There is also an open arrow pointing to a regular melt pool, which can be found in both planes and is actually a cross-section of a laser track going in the y-direction.
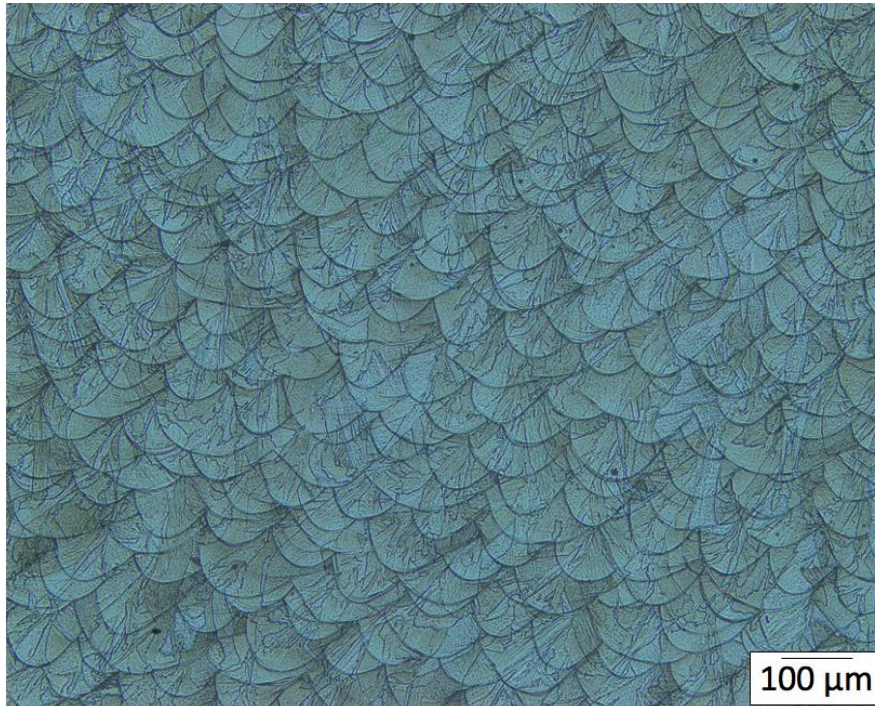
Figure 27: Image of the structure in the yz-plane (S2).

When looking at Figure 27 it does seem like there are more fusion lines in this plan due to the lack of longitudinal laser tracks, thus meaning that there are more barriers in addition to the grain boundaries for the dislocations to possibly have to move past. This would mean that the tensile strength, ductility and hardness should be higher for y-oriented specimens. Which happens to be the case by recalling that the hardness in the yz- plane (S2) was 222.6 compared to a hardness of 204.6 in the xz-plane (S3) and that specimen YY exhibited a higher tensile strength and elongation than XX. Therefore, it can be said that the microstructure corresponds with the mechanical test results. Mentioning the hardness results it should be said that they are also in agreement with the results from the Tec Eurolab and are very similar to those of the regular powder.

6.1.4 Impact toughness

The toughness of a material can be ascertained from the strain vs stress curve by looking at the area under the curve until fracture where a lower area indicates low strength and ductility, but high toughness. Calculations show that specimen XX has a distinctively lower area than the other specimens. Specimen YY follows next, but the z-oriented specimens follow closely after. This would mean that the x-specimens should exhibit the highest toughness and the z-specimens the lowest. By looking at the impact results it can be seen that this is very much the case. Table 6 is repeated below for practicality.

ORIENTATION	AVERAGE	MAX	MIN	SD
X	99.6	101.6	98.3	1.4
Y	82.7	84.2	80.6	1.5
Z	71.2	76.4	67.4	3.8

As a short note it can be mentioned that the results from Tec Eurolab are very consistent with the results of this study, but only y- and z-specimens can be compared because the x-specimens of Tec Eurolab had different dimensions. It can also be mentioned that in their testing the z-specimens exhibited higher toughness than the y-specimens did despite being very close as in this study. This is very reasonable and could have been the case in this study with regards to the area under the curves of y- and z-specimens being very close. It is also mentionable that the results from the master study are quite higher than those of this study where especially the z-specimens sticks out because they exhibited twice as much. However, the specimens of the master study were machined without cooling in order to reach the correct dimensions, but the specimens of this study were not machined except for the notch. Therefore, the results are not entirely comparable though the least machined samples are the z-specimens where the greatest difference is. More investigation as well as the results from the other study would be needed in order to give an explanation to the differences. When trying to give an explanation to why the x-specimens of this study exhibited much higher toughness than the other specimens of this study. One could only speculate that during the impact, the dislocation was allowed to move along the longitudinal laser tracks shown in Figure 26 at a low energy cost compared to the dislocations in the other specimens which most likely were stopped by a fusion line. In order to give a more complete explanation, the fractured surfaces would need to be examined by the use of a Scanning Electron Microscopic (SEM) in order to determine what kind of fracture that took place. This was not possible during this study due to circumstances.

6.2 Microstructural assessment

As of the Scanning Electron Microscope (SEM) image seen in Figure 29 the particles seem to have a fairly spherical shape and the number of satellites seems to be low. The particles have an average size of 34.30 µm. Aidro has not mentioned any problem during the printing of the specimens and it is therefore fair to assume that the other properties of the powder are as desired. It is also worth mentioning that no unmelted powder was discovered during light optical examination.
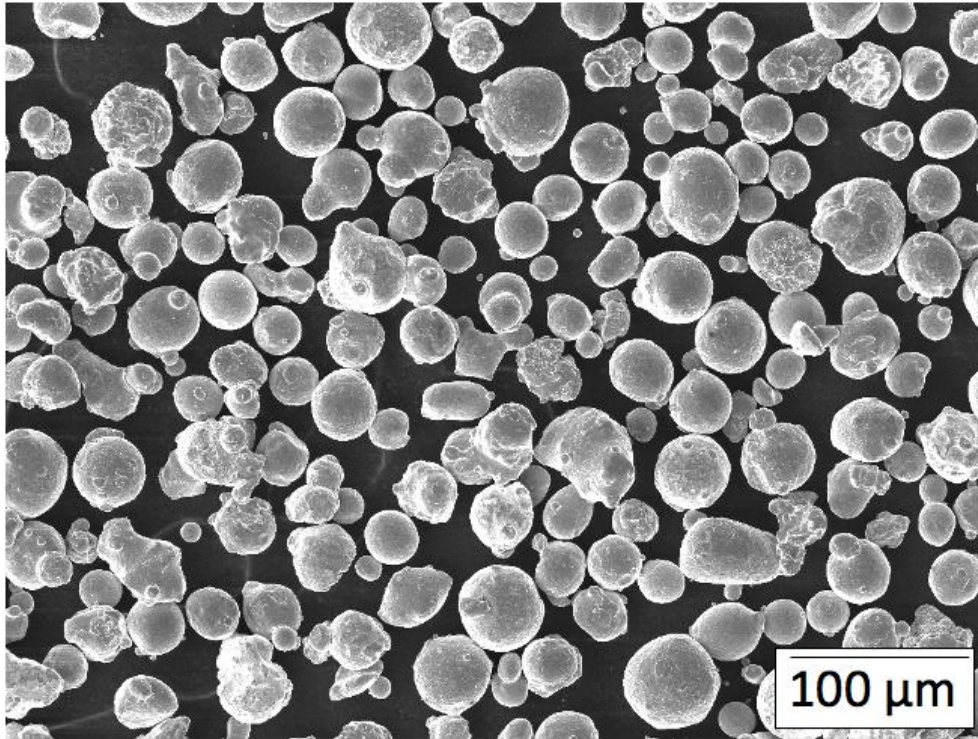
Figure 28: SEM image 316L "green" powder provided by F3nice.

6.2.1 Characteristics of the grain growth

Conceivable should the width of the melt pools correspond to the width of the previously mentioned laser tracks, which they in some degree do. However, the melt pools do not inhabit their original sizes due to the fact that they have been partially remelted during the formation of the layer above. The partial remelting can be seen by some of the melt pools almost overlapping each other, indicated by the black arrows in Figure 23, which is repeated for practical considerations. In fact, overlapping makes the layers bind better together and the fact that overlapping can be seen in structure is a good indication of the properties of the powder being as could be expected.
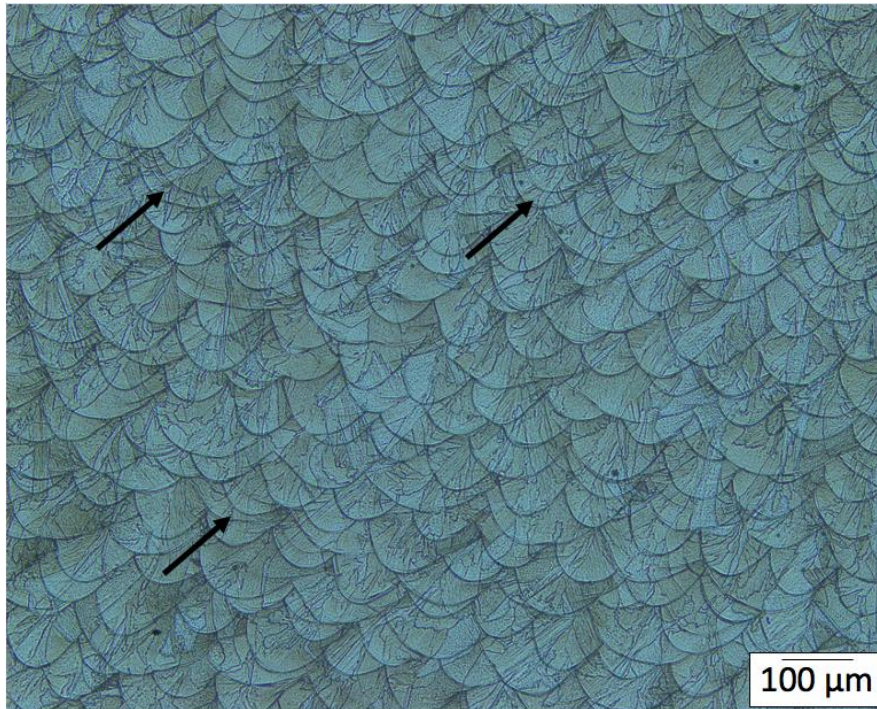
The partial remelting of the melt pools is also the cause of epitaxial grain growth by allowing new solid material to form by keeping the same crystallographic of the nearby grains. The result is a stronger bond between layers. In previous studies it has been reported that Selective Laser Melting (SLM) is able to produce texture and preferred crystallographic orientation of grains along the building direction. In order to prevent formation of a too intense texture in both the building and the horizontal direction a scanning pattern which rotates about 50° has been introduced. Thus, resulting in a highly isotropic structure. Though it has to mentioned that the remelting may cause residual stress to build up or any defect to form between the layers. Which can potentially explain the lower properties in the z-direction. Further it can be shown that grain growth past the fusion line was found in another study investigating 316L produced by SLM (Tucho et al., 2018).
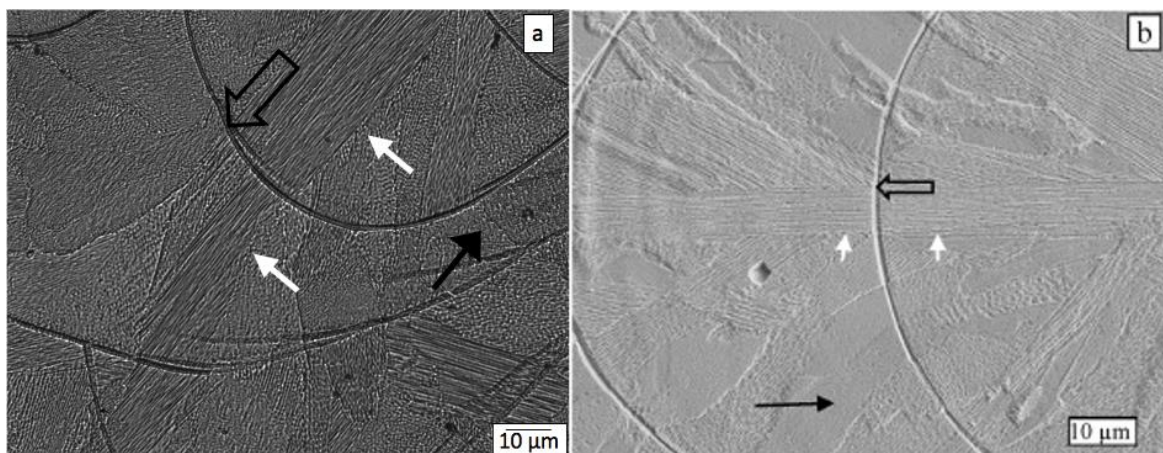
Figure 29: a) Optical microscopy from this study (S2), b) SEM (Tucho et al., 2018). The white arrows indicate example of columnar grains that cross the fusion line. Growth direction is shown with black arrows while fusion line is indicated with open arrows.

45

As can be seen in Figure 29 (b) did the other study point out columnar grains growing past the fusion line and by the look of the grain in Figure 29 (a) it can be assumed that this is also a columnar grain. Thereby, a columnar grain can be seen in both cases growing past the fusion line. Thus, indicating that some of the same grain growth has happened in the samples of this study as in the samples of the other study. Again, indicating that the properties of the powder are as they could be expected to be. To further strengthen the indication of grain growth happening as could be expected, an image from yet another study (Casati et al., 2016) can be seen in Figure 30 (b). However, in this image grains growing in all directions is depicted alongside an image of grains also growing in all directions in the yz-plane of a sample from this study seen in Figure 30 (a).
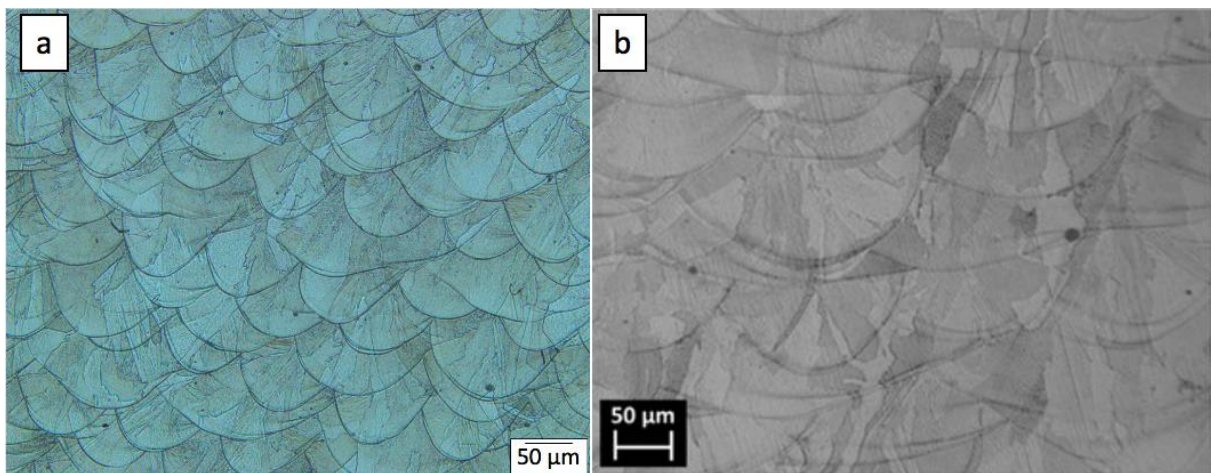
Figure 30: a) Optical microscopy from this study (S2), b) Optical micrograph of the lateral of built parts (Casati et al., 2016)

6.2.2 Porosity assessment

The examination of the surfaces of samples S1, S2, S3 and E showed as seen earlier that the porosity is very low. Though desirable it should be at zero, but unless other is specified the DNVGL-ST-B203 allows for a maximum pore content of 0.5% which the pore content found in this study is well below by the highest average content found on a surface being 0.37%. However, Tec Eurolab found the average metal percentage to be 99.9% giving a pore content of 0.01%, which is significantly lower than what was found in this study. This difference could probably be caused by that fact that the samples of this study was etched before the light optical microscopic images of the structure were taken. Though the samples were polished again before porosity assessment, the polishing may not have been able to remove the entire effect the etching had on the surface. Thus, leaving a larger number of pores than it should originally be.

7 Conclusion

The objective of this study has been to investigate if 316L powder for Selective Laser Melting (SLM) can be made from scrap material by the process of Vacuum Induction Gas Atomizing (VIGA) and thus lowering the cost of raw materials, energy used, and emissions emitted compared to the traditional production cycle. Thereby also making it more sustainable to incorporate the high energy demanding SLM process into a circular economy. The question in mind during this study has been whether there would be any impact from the potential presence of contaminants. As of the results it where detected that there could be a larger amount of certain elements, explaining some of the difference in the results. However, the effect of contaminants was mentioned in the introduction and is a well-known dilemma with regards to recycling. If a circular economy were to be incorporated a great approach when designing a new part would be to design the part with a view to recycling the part at the end of its lifetime, in order to prevent unwanted elements in the chemistry.

Further, as the investigation of the microstructure has shown that the microstructure exhibited similar characteristics found in other studies studying SLM manufactured 316L specimens and the correspondence between the mechanical properties and the microstructure has been shown as well. Some of the observed similarities include observations of overlapping melt pools due to partially remelting, what is believed to be epitaxial grain growth as well as grains growing in no preferred direction. Thus, indicating that the laser scanning pattern has successfully manage to create isotropic like conditions in the microstructure.

The mechanical testing has shown that the specimens examined in this study exhibits mechanical properties well within the requirements of the relevant standard, though exhibiting slightly lower properties than the specimens produced by regular powder. However, a lower performance in the z-direction could be observed in this study as well in the master study. Therefore, as a result this study has made it possible to make the conclusion that it is feasible to produce 316L powder. suitable for Selective Laser Melting (SLM) by the use of scrap material as the main input material when producing powder by Vacuum Induction Gas Atomizing (VIGA).

8 References

Alfajern. (2020). In *Store norske leksikon*.

ASTM International. (2016). *Standard specification for additive manufacturing stainless steel alloy (UNS S31603) with powder bed fusion* (Vols. F3184-16). ASTM International.

Bratkovich, S., Fernholz, K., Frank, M., Groot, H., & Howe, D. J. (n.d.). *UNDERSTANDING STEEL RECOVERY AND RECYCLING RATES AND LIMITATIONS TO RECYCLING*. 12.

Cacace, S., Furlan, V., Sorci, R., Semeraro, Q., & Boccadoro, M. (2020). Using recycled material to produce gas-atomized metal powders for additive manufacturing processes. *Journal of Cleaner Production*, *268*, 122218.

Casati, R., Lemke, J., & Vedani, M. (2016). Microstructure and Fracture Behavior of 316L Austenitic Stainless Steel Produced by Selective Laser Melting. *Journal of Materials Science & Technology*, *32*(8), 738–744.

Damuth, R. J. (2011). *Estimating the Price Elasticity of Ferrous Scrap Supply*. 26. González-Viñas, W., & Mancini, H. (2003). *Science of Materials: An Introduction (Pre-print)*.

Grønnere – Stålproduksjon i dag. (n.d.). Grønnere – Stålproduksjon i dag. Retrieved March 11, 2021

Guo, Y., Lu, W.-F., & Fuh, J. (2021). Semi-supervised deep learning based framework for assessing manufacturability of cellular structures in direct metal laser sintering process. *Journal of Intelligent Manufacturing*, *32*.

Knowles, C., Becker, T., & Tait, R. (2012). Residual stress measurements and structural integrity implications for selective laser melted TI-6AL-4V. *South African Journal of Industrial Engineering*, *23*, 119–129.

Limitations of Optical Microscopy. (2017, April 10). News-Medical.Net.
Metal powders for AM: Manufacturing processes and properties. (2018, June 1). Metal Additive Manufacturing.

Nondestructive Evaluation Physics: Materials. (n.d.). Retrieved May 20, 2021

Priarone, P. C., Ingarao, G., Lunetto, V., Di Lorenzo, R., & Settineri, L. (2018). The Role of re-design for Additive Manufacturing on the Process Environmental Performance. *Procedia CIRP*, *69*, 124–129.

Sedriks, A. J. (1996). *Corrosion of stainless steels* (2nd ed.). Wiley.

Shifeng, W., Shuai, L., Qingsong, W., Yan, C., Sheng, Z., & Yusheng, S. (2014). Effect of molten pool boundaries on the mechanical properties of selective laser melting parts. *Journal of Materials Processing Technology*, *214*(11), 2660–2667.

Smith, W. F. (1993). *Structure and properties of engineering alloys* (2nd ed.). McGraw-Hill. *Stainless Steel and CO2: Facts and Scientific Observations*. (n.d.). 12.

The Stainless Steel Family. (n.d.). 5.

Tucho, W. M., Lysne, V. H., Austbø, H., Sjolyst-Kverneland, A., & Hansen, V. (2018). Investigation of effects of process parameters on microstructure and hardness of SLM manufactured SS316L. *Journal of Alloys and Compounds*, *740*, 910–925.

Urionabarrenetxea, E., Avello, A., Rivas, A., & Martín, J. M. (2021). Experimental study of the influence of operational and geometric variables on the powders produced by close-coupled gas atomisation. *Materials & Design*, *199*, 109441.

Wallner, S. (2019). Powder Production Technologies. *BHM Berg- Und Hüttenmännische Monatshefte*, *164*(3), 108–111.

Wang, M. R., & Chen, P. J. (n.d.). *Mechanism and Performance of a Novel Atomizer for Metal Powder Production with Supersonic Configuration*. 5.

Worldsteel | worldsteel. (n.d.). Retrieved March 11, 2021

Tensile result of every tensile specimen.

ORIENTATION	SPECIMEN NAME	YS 0.2% (MPA)	UTS (MPA)	EL (%)	RA (%)	E (GPA)
X	X	519.3	619.1	31.2	62.4	110
Y	Y	541.9	631.1	33.1	62.1	134
Z	A	457.4	559.6	38.9	63.2	109.2
	B	451.8	561.1	38.7	61.7	109.7
	C	456.1	546.4	37.8	64.3	98.9
	D	455.8	549.4	39.5	63.5	102.2
	E	458.1	554.3	37.8	65.0	97.9

YS – Yield Strength, UTS – Tensile Strength, EL, Elongation, RA – Reduction of Area and

E – E-modulus/Young's modulus

Impact result of every impact specimen.

Specimen	Result (J)
XX1	99.0
XX2	98.3
XX3	101.6
YY1	83.2
YY2	80.6
YY3	84.2
ZZ1	69.7
ZZ2	67.4
ZZ3	76.4

Appendix B / Hardness data

Hardness data from all three samples. On the samples S1, S2, S3 six, nine and eleven measurement were taken respectively, giving a total of 26 measurements.

NUMBER OF MEASUREMENT	S1	S2	S3
1	211.6	221.1	209.2
2	218.4	219.3	203.1
3	217.7	217.0	210.6
4	219.4	216.1	206.3
5	208.6	225.1	208.2
6	213.1	218.7	206.9
7		232.5	204.2
8		219.1	207.7
9		234.9	203.4
10			195.7
11			195.5

Appendix C / Tec Aurolab test report

<table>
<tr><td rowspan="2">🧪 TEC·Eurolab
we make you feel sure</td><td>Rapporto di Prova
Test Report</td><td>21-02974-01
Pag. 1 di 2</td><td>Data
Date</td><td>30/04/2021</td></tr>
<tr><td>Committente
Customer</td><td colspan="3">EIT MANUFACTURING ASBL
VIA ROCCOLI 252
23010 PIANTEDO - SO</td></tr>
</table>

Vostro riferimento / Reference	Rif DDT A MANO del 22/04/2021
Ordine di acquisto/Purchase Order	
Campione / Sample [1]	AB,BB,CB,DB,EB,xx,yy
Descrizione / Description [1]	SPECIMENS for tensile test - Mat. Stainless Steel 316L
Data ricevimento / Receiving date	22/04/2021
Ns. codice campione / Sample code	21-02974 01-01,01-02,01-03,01-04,01-05,01-06,01-07
Prova richiesta / Test	TENSILE TESTING RT METHOD ASTM E8/E8M
Luogo esecuzione prova / Test place	Viale Europa 40-41011 Campogalliano MO
Data inizio prova / Test start date	29/04/2021
Data fine prova / Test end date	29/04/2021

TRAZIONE A TEMPERATURA AMBIENTE
MATERIALI METALLICI FERROSI E NON FERROSI
TENSILE TEST AT ROOM TEMPERATURE
FERROUS AND NON-FERROUS METALLIC MATERIALS

PROVA ACCREDITATA ACCREDIA / ACCREDIA ACCREDITED TEST

Metodo di Prova / Test Method: PDP 017 Rev 36

Norma di Prova / Test Standard: ASTM E8 Rev 21

Strumentazione / Equipment:
Dinamometro / Dynamometer ("PM04") Zwick Roell Z600

Campionamento / Sampling: Effettuato dal committente / Performed by the customer

Ulteriore documentazione applicabile / Additional applicable documentation: n.a.

Condizioni ambientali di prova garantiti dal laboratorio/ Environmental test conditions guaranteed by the laboratory:
Intervallo di Temperatura/Temperature Range: T=23±3°C
Intervallo di Umidità Relativa/Relative Humidity Range: U<60%

Provetta Test Specimen	Specimen 3 Fig. 8 ASTM E8 Rev 21	Prelievo Sampling	Effettuato dal committente Performed by the customer	Metodo Method	C

Firmato digitalmente da : VERZELLONI DAVIDE - Responsabile di Commessa

ilac-MRA

ACCREDIA
L'ENTE ITALIANO DI ACCREDITAMENTO
LAB N° 0052 L

TEC·Eurolab
we make you feel sure

Specimen ID	D mm	S_0 mm²	G mm	TS MPa	$Y_{0.2}$ MPa	E at fracture %	Z %
SPECIMENS for tensile test - Mat. Stainless Steel 316L AB	6,00	28,3	24	563	466	49,0	66
SPECIMENS for tensile test - Mat. Stainless Steel 316L BB	5,99	28,2	24	565	468	49,5	67
SPECIMENS for tensile test - Mat. Stainless Steel 316L CB	5,99	28,2	24	552	464	48,5	65
SPECIMENS for tensile test - Mat. Stainless Steel 316L DB	6,00	28,2	24	552	463	51,5	68
SPECIMENS for tensile test - Mat. Stainless Steel 316L EB	5,99	28,2	24	560	467	48,0	65
SPECIMENS for tensile test - Mat. Stainless Steel 316L xx	5,99	28,2	24	628	530	38,5	65
SPECIMENS for tensile test - Mat. Stainless Steel 316L yy	5,99	28,1	24	638	549	39,5	62

LEGENDA:

- **D**: diametro provino / specimen diameter
- **S_0**: sezione trasversale / cross-sectional area
- **G**: tratto utile / gage length
- **TS**: carico massimo / ultimate tensile strength
- **$Y_{0.2}$**: carico di snervamento (scostamento 0,2%) / yield strength (offset 0,2%)
- **E at fracture**: allungamento a rottura / elongation at fracture
- **Z**: strizione / reduction of area

Il Responsabile della Prova
P.I CONVERSO DAVIDE

[signature]

	Rapporto di Prova Test Report	21-02974-02 Pag. 1 di 2	Data Date	30/04/2021
TEC·Eurolab we make you feel sure	Committente Customer	**EIT MANUFACTURING ASBL** VIA ROCCOLI 252 23010 PIANTEDO - SO		

Vostro riferimento / Reference	Rif DDT A MANO del 22/04/2021
Ordine di acquisto/Purchase Order	
Campione / Sample [1]	xx1 - xx2 - xx3,yy1 - yy2 - yy3,zz1 - zz2 - zz3
Descrizione / Description [1]	SPECIMENS for impact test - Mat. Stainless Steel 316L
Data ricevimento / Receiving date	22/04/2021
Ns. codice campione / Sample code	**21-02974** 02-01,02-02,02-03
Prova richiesta / Test	IMPACT TEST RT 3 SPECIMEN METHOD ASTM E23
Luogo esecuzione prova / Test place	Viale Europa 40-41011 Campogalliano MO
Data inizio prova / Test start date	29/04/2021
Data fine prova / Test end date	29/04/2021

<div align="center">

PROVA DI RESILIENZA A TEMPERATURA AMBIENTE
IMPACT TEST AT ROOM TEMPERATURE
PROVA ACCREDITATA ACCREDIA / ACCREDIA ACCREDITED TEST

</div>

Metodo di Prova / Test Method: PDP 015 Rev 27
Norma di Prova / Test Standard: ASTM E23 Rev 18
Strumentazione / Equipment: Pendolo Charpy / Charpy pendulum ("PR03") Zwick/Roell RKP450
Campionamento / Sampling: Effettuato dal committente / Performed by the customer
Ulteriore documentazione applicabile / Additional applicable documentation: n.a.
Condizioni ambientali di prova garantiti dal laboratorio/ Environmental test conditions guaranteed by the laboratory: Intervallo di Temperatura/Temperature Range: T=18÷25°C Intervallo di Umidità Relativa/Relative Humidity Range: U<60%
Dimensioni provetta / Specimen dimension: 7,5 x 10 x 55 mm
Temperatura di prova / Test temperature: Temperatura ambiente/Room Temperature
Tipo di intaglio / Notch type: V profondità 2 mm / V cut depth 2 mm
Prelievo / Sampling: Effettuato dal committente / Performed by the customer

Campione	KV_8 (J)	Media (J)
xx1 - xx2 - xx3	71-73-73	72

<div align="center">

Rottura avvenuta per tutte le provette sottoposte a prova
All specimens tested were broken

</div>

Firmato digitalmente da: VERZELLONI DAVIDE - Responsabile di Commessa

V

PROVA DI RESILIENZA A TEMPERATURA AMBIENTE
IMPACT TEST AT ROOM TEMPERATURE
PROVA ACCREDITATA ACCREDIA / ACCREDIA ACCREDITED TEST

Metodo di Prova / Test Method: PDP 015 Rev 27

Norma di Prova / Test Standard: ASTM E23 Rev 18

Strumentazione / Equipment:
Pendolo Charpy / Charpy pendulum ("PR03") Zwick/Roell RKP450

Campionamento / Sampling: Effettuato dal committente / Performed by the customer

Ulteriore documentazione applicabile / Additional applicable documentation: n.a.

Condizioni ambientali di prova garantiti dal laboratorio/ Environmental test conditions guaranteed by the laboratory:
Intervallo di Temperatura/Temperature Range: T=18÷25°C
Intervallo di Umidità Relativa/Relative Humidity Range: U<60%

Dimensioni provetta / Specimen dimension: 10 x 10 x 55 mm

Temperatura di prova / Test temperature: Temperatura ambiente/Room Temperature

Tipo di intaglio / Notch type: V profondità 2 mm / V cut depth 2 mm

Prelievo / Sampling: Effettuato dal committente / Performed by the customer

Campione	KV_8 (J)	Media (J)
yy1 - yy2 - yy3	72-72-70	71
zz1 - zz2 - zz3	80-76-78	78

Rottura avvenuta per tutte le provette sottoposte a prova
All specimens tested were broken

Il Responsabile della Prova
P.I CONVERSO DAVIDE

Vostro riferimento / Reference	Rif DDT A MANO del 22/04/2021
Ordine di acquisto/Purchase Order	
Campione / Sample (1)	CB, CB20
Descrizione / Description (1)	SPECIMENS for tensile test - Mat. Stainless Steel 316L,SPECIMEN
Data ricevimento / Receiving date	22/04/2021
Ns. codice campione / Sample code	21-02974 01-03-01,03-01-02
Prova richiesta / Test	VICKERS HARDNESS METHOD ISO 6507-1 (su cubo e su cilindro)
Luogo esecuzione prova / Test place	Viale Europa 40-41011 Campogalliano MO
Data inizio prova / Test start date	30/04/2021
Data fine prova / Test end date	30/04/2021

PROVA DI DUREZZA VICKERS
VICKERS HARDNESS TEST

PROVA ACCREDITATA ACCREDIA / ACCREDIA ACCREDITED TEST

Metodo di Prova / Test Method: PDP 013 Rev 21	Norma di Prova / Test Standard: UNI EN ISO 6507-1 Rev 2018

Ulteriore documentazione applicabile / Additional applicable documentation: N.A.

Strumentazione / Equipment: Durometro / Hardness Testing Machine ("DU14") KB PRUFTECHNIK – KB250 – S20-2-846-2168

Campionamento / Sampling: Effettuato dal committente / Performed by the customer

Condizioni ambientali di prova garantiti dal laboratorio/ Environmental test conditions guaranteed by the laboratory: Intervallo di Temperatura/Temperature Range: T~23±3°C; Intervallo di Umidità Relativa/Relative Humidity Range: U<60%

La prova è stata eseguita a cuore sulla sezione longitudinale del componente CB. / The test was performed at core on the longitudinal section of the sample CB.

	CB	CB20
Scala / Scale	Vickers, HV10	Vickers, HV10
Penetratore / Indenter	Piramide di diamante / Diamond pyramid	Piramide di diamante / Diamond pyramid
Carico / Load	10 kg (98,07 N)	10 kg (98,07 N)
Letture / Readings	(200-210-206) HV	(210-208-205) HV
Risultato (valore medio) / Result (average value)	205 HV	208 HV

Il Responsabile della Prova / Test Responsible
Dott. BARANI SIMONE

ilac-MRA

ACCREDIA
L'ENTE ITALIANO DI ACCREDITAMENTO
LAB N° 0052 L

Vostro riferimento / Reference	Rif DDT A MANO del 22/04/2021
Ordine di acquisto/Purchase Order	
Campione / Sample (1)	CB20
Descrizione / Description (1)	SPECIMEN
Data ricevimento / Receiving date	22/04/2021
Ns. codice campione / Sample code	21-02974 03-01
Prova richiesta / Test	DENSITY BY WATER DISPLACEMENT METHOD ASTM B311
Luogo esecuzione prova / Test place	Viale Europa 40-41011 Campogalliano MO
Data inizio prova / Test start date	28/04/2021
Data fine prova / Test end date	29/04/2021

MISURA DELLA DENSITA' ALLA BILANCIA IDROSTATICA DENSITY BY IMMERSION METHOD
Metodo di Prova / Test Method: MI 081 Rev 0
Norma di Prova / Test Standard: ASTM B311 Rev 17
Strumentazione / Equipment: Bilancia idrostatica ("BL10") Metler Toledo ME
Campionamento / Sampling: Effettuato dal committente / Performed by the customer
Ulteriore documentazione applicabile / Additional applicable documentation: N.A.
Condizioni ambientali di prova garantiti dal laboratorio/ Environmental test conditions guaranteed by the laboratory: Intervallo di Temperatura/Temperature Range: T=23±3°C Intervallo di Umidità Relativa/Relative Humidity Range: U<60%
Stato fisico del campione/Physical state of the sample: Solido massivo
Trattamenti-Detrattamenti/ Treatment-detreatment: N.A.

Sul campione ricevuto è stata determinata la densità mediante bilancia idrostatica.

The density of received sample was determined with a hydrostatic balance

	Density (g/cm³)
CB20 SPECIMEN	7,96

Il Responsabile della Prova
Dott. MARZANI LUCA

[firma]

Firmato digitalmente da: VERZELLONI DAVIDE - Responsabile di Commessa

TEC·Eurolab we make you feel sure	Rapporto di Prova Test Report	21-02974-05 Pag. 1 di 4	Data Date	30/04/2021
	Committente Customer	EIT MANUFACTURING ASBL VIA ROCCOLI 252 23010 PIANTEDO - SO		

Vostro riferimento / Reference	Rif DDT A MANO del 22/04/2021
Ordine di acquisto/Purchase Order	
Campione / Sample (1)	CB20
Descrizione / Description (1)	SPECIMEN
Data ricevimento / Receiving date	22/04/2021
Ns. codice campione / Sample code	21-02974 03-01-01
Prova richiesta / Test	DENSITY BY MICROGRAPHIC EXAMINAT. (ESTIMATION OF POROSITY) METHOD VDI 3405-2
Luogo esecuzione prova / Test place	Viale Europa 40-41011 Campogalliano MO
Data inizio prova / Test start date	30/04/2021
Data fine prova / Test end date	30/04/2021

DETERMINAZIONE DELLA DENSITÁ PER VIA MICROGRAFICA (STIMA DEL CONTENUTO DI VUOTI)
DETERMINATION OF DENSITY BY MICROGRAPHIC EXAMINATION (ESTIMATION OF POROSITY)

Metodo di Prova / Test Method: N.A.	Norma di Prova / Test Standard: N.A.

Ulteriore documentazione applicabile / Additional applicable documentation: VDI 3405-2

Strumentazione / Equipment: Microscopio ottico / Light Microscope Zeiss AXIO ("MS07")

Campionamento / Sampling: Effettuato dal committente / Performed by the customer

Condizioni ambientali di prova garantiti dal laboratorio/ Environmental test conditions guaranteed by the laboratory:
Intervallo di Temperatura/Temperature Range: T=23±3°C; Intervallo di Umidità Relativa/Relative Humidity Range: U<60%

La prova è stata effettuata su un provino ottenuto da una sezione trasversale del campione in oggetto, montato in resina e opportunamente lucidato.
La percentuale di vuoti è stata stimata mediante osservazione delle sezioni lucidate impiegando un software di analisi dell'immagine, e sfruttando quindi il massimo contrasto tra metallo (tonalità chiara) e vuoti (tonalità scura).
Le modalità di esecuzione della prova e risultati ottenuti sono mostrati nelle pagine seguenti.

The test was performed on a metallographic specimen obtained by cross-cut section of the sample.
After being resin mounted and polished, the percentage of voids was estimated observing the polished sections and using an analysis software, exploiting the maximum contrast between metal (light shade) and voids (dark shade).
The methods of execution of the test and the results obtained are shown on the following pages.

Il Responsabile della Prova / Test Responsible
Dott. BARANI SIMONE

TEC·Eurolab
we make you feel sure

La stima del contenuto di vuoti è stata effettuata mediante osservazione di N.5 campi a 50X di ingrandimento, scelti al fine di rendere statisticamente rilevante, confrontabile e riproducibile l'analisi, così come richiesto dal committente e di seguito mostrato:

Di ciascun campo (la cui dimensioni è circa 1,5 mm x 2,0 mm) è stata valutata la percentuale di vuoti e ne viene fornita la documentazione fotografica.
Successivamente è stata individuata visivamente la porosità peggiore. Ne viene indicata la posizione sul provino e la dimensione lineare massima.

I risultati sono mostrati nelle pagine seguenti.

————————————————

The percentage of voids was estimated observing N.5 fields at a 50x magnification, chosen in order to make the analysis statistically relevant, comparable and reproducible, as requested by the client and shown below:
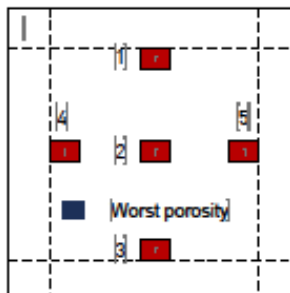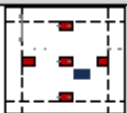
For each field (dimension about 1,5 mm x 2,0 mm) the percentage of voids was estimated and the photographic documentation is provided.
Subsequently the worst porosity has been identified and its photo and maximum linear dimension are indicated.

Firmato digitalmente da: VERZELLONI DAVIDE - Responsabile di Commessa

X

Campione Sample	Percentuale pieno valori (%) da 1 a 5 Metal Percentage (%) From field 1 to 5	Percentuale pieno valore medio Average Metal Percentage	Porosità Peggiore / Worst Porosity	
			Dimensione Dimension	Posizione Position
SPECIMEN CB20 (Foto / Photo N.1)	99,9-99,9-99,9-99,9-99,9	> 99,9%	25 µm	

Firmato digitalmente da : VERZELLONI DAVIDE - Responsabile di Commessa

FOTO/Photo N. 1.　　　　　　　　　　**SPECIMEN CB20**

Campo / Field 1	Campo / Field 2
500 µm	500 µm
Campo / Field 3	Campo / Field 4
500 µm	500 µm
Campo / Field 5	Porosità peggiore / Worst porosity – 100x
500 µm	200 µm

Firmato digitalmente da : VERZELLONI DAVIDE - Responsabile di Commessa